NORTHWESTERN UNIVERSITY


**Finite Element Analysis of TDR Cable-Grout-Soil Mass Interaction During Localized Shearing**


A Thesis
Submitted to the Graduate School
In Partial Fulfillment of the Requirements
For the Degree
MASTER OF SCIENCE
Field of Civil Engineering


By
James Tanner Blackburn


EVANSTON, ILLINOIS
April, 2002

## **Acknowledgements**

I would like to acknowledge the individuals and organizations that made it possible to complete this thesis. Financial support was provided by the U.S. Department of Transportation funded Infrastructure Technology Institute of Northwestern University and the National Science Foundation. Dr. Charles Dowding was the advisor for this thesis and I thank him for the guidance and assistance. Dr. Richard Finno also provided insight and advice for this project, which I greatly appreciate. Also, Dr. Raymond Krizek served on the review committee for this thesis, and I thank him for this. Previous theses completed by Richard Cole, Charlie Pierce, and other previous TDR graduate students in the Geotechnical program provided valuable information and insight.

I would also like to thank the entire geotechnical engineering graduate student group for the support and encouragement during the past two years; with special appreciation to Jill Roboski, Michele Calvello, and Laureen McKenna for their outstanding friendship. Lastly I would like to thank my family, both here in Chicago and in Leucadia, for their support.

# Table of Contents

## List of Figures

## List of Tables

# Chapter 1.  <u>Introduction</u>

This thesis combines field and laboratory measurements with three dimensional (3D) finite element analysis (FEM) to demonstrate the use of Time Domain Reflectometry (TDR) cable-grout composites to measure localized shearing in soft soil. Past field installations of TDR cable-grout composites in rock have lead to its widespread use in the mining industry (Dowding and Huang, 1994).  Lack of well instrumented installations in soil as well as differences in failure mechanisms and relative stiffnesses of rock and soil have inhibited development of optimal cable-grout composites for soil.

A deforming landfill on soft clay provided an opportunity to field test the response of two different TDR cable-grout composites in soft soil.  TDR signal reflections from the more compliant of the cable-grout composites in the field test shows that TDR cable-grout systems can be devised to respond to localized shearing in soil. However, additional analysis of the interaction between the cable, grout, and soil mass is required for design of TDR cable-grout composites employed in soft soils.

Three dimensional (3D) finite element modeling (FEM) is employed to leverage field and laboratory measurements to analyze the interaction of a wide range of cable-grout inclusions and surrounding soil masses.  Necessary model properties of cable, grout, and cable-grout interfaces were first back-calculated via 3D FEM from laboratory measurements of cable and cable-grout composite response to shearing.  These back-calculated properties were then employed to extend the modeling to include the full interaction of cable, grout, and soil-mass.  This complete model was then exercised to

investigate a suite of cables, grouts, and soils with variable strengths and stiffnesses to establish an optimum cable-grout composite design for a given soil.

Analysis of TDR cable-grout-soil interaction is presented in the following order: 1) discussion of field case study, 2) comparison of laboratory results of shearing of individual cables and cable-grout composites with three dimensional finite element model results, and 3) employment of three dimensional finite element models to analyze cable-grout-soil interaction of TDR composites placed in soft to medium soils.

# Chapter 2.  <u>Shear Failure Detection and Monitoring Using Time Domain Reflectometry</u>

A deforming landfill on soft clay provided an opportunity to field test the response of two different Time Domain Reflectometry (TDR) cable-grout composites in soft soil.  Past field test installations of TDR cable-grout composites in rock have lead to widespread use of the technology in the mining industry (Dowding and Huang, 1994).  However, a dearth of well instrumented installations in soil, as well as differences in failure mechanisms and relative stiffness of rock and soil have inhibited development of optimal cable-grout composites for soil.  Thus there are fewer installations in soil.  Results of this case study and the finite element study of composite inclusions in soil in subsequent chapters, establish the background necessary for the application of TDR cable measurement of localized deformation in soil as a supplement to slope inclinometers.

Two TDR cable-grout composites were installed near two slope inclinometers (SI) in the deforming fill and responses of the two systems were recorded over a period of over two years.  TDR signal reflections from one of the cable-grout composites in the field test show that composite TDR cable-grout systems can be devised to respond to localized shearing in soil.

## *Monitoring of Localized Shear Failure in Soft Clay*

Localized shear failure in soft clays was monitored with both slope inclinometers and TDR cable-grout composites to compare responses.  Data were collected for nearly two years.  The combination of inclinometer and TDR responses allowed determination of likely boundaries of the shear zone, as well as measurement of total shear deformation.

Slope failure occurred with some 30 to 50 feet of stiff, fill material, placed on 3 feet of silt and sand overlying 40 to 50 feet of soft glacial clay. As shown in Figure 2-1, localized shear failure occurs in the soft clay layer, at a depth of 90 to 100 feet, at the location of Cable A.

Two different TDR cable-grout composites were installed in the landfill. A 22 millimeter, solid aluminum outer conductor cable (Cable A) was installed near the right slope inclinometer (Inclinometer 1 in Figure 2-1), while a 10 mm, braided outer conductor cable (Cable B) was installed near the left inclinometer (Inclinometer 2). Both TDR cables were grouted in approximately 10 centimeter diameter boreholes. Details of the cable-grout composite placed in the failing soil are presented in Table 2-1. Cable type, cable stiffness, and grout strength varied significantly. The high water/cement ratio of the grout for the solid aluminum outer conductor cable leads to much lower grout strength, and thus stiffness, for that composite.
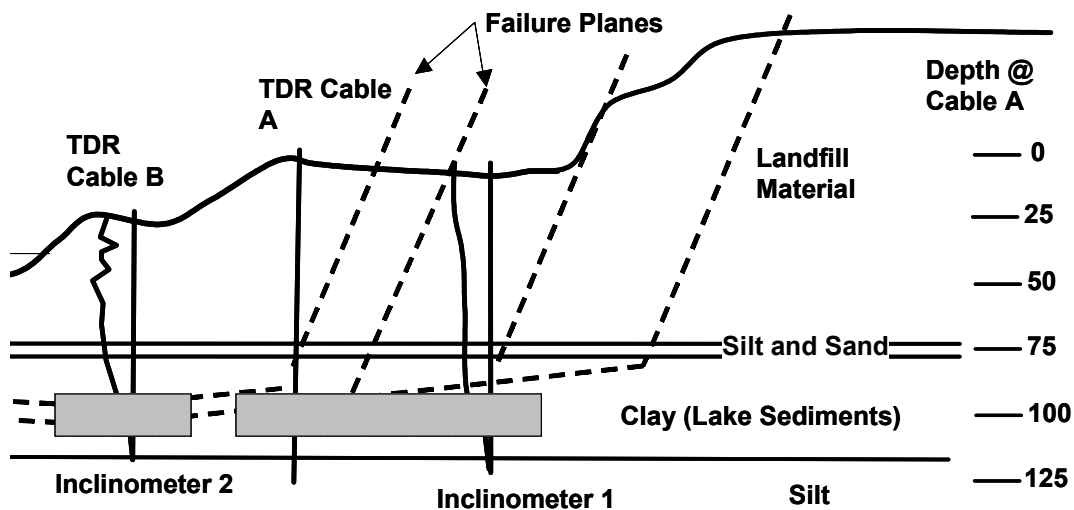
**Figure 2-1. Landfill Soil Profile, Shear Failure Locations and Instrumentation Locations.**

| Composite Properties of Field Cables | | |
|---|---|---|
| Property | Values | |
| Cable Outer Conductor Material | Solid Aluminum | Braided Copper |
| Cable Diameter [mm] | 22 | 8 |
| Cable Stiffness, $EI^1$, [kN-m$^2$] | 0.266 | 0.000122 |
| Hole Diameter [mm] | 98 | 100 |
| Grout Contents | | |
| Cement [%] | 33 | 50 |
| Water [%] | 65 | 48 |
| Bentonite [%] | 2 | 2 |
| Grout Strength, $q_u$ $^2$ [kPa] | 500 | 3900 |
| Composite Stiffness, EI, [kN-m$^2$] | 0.725 | 2.46 |
| Cable Type $^3$ (Brand) | Commscope  PIII-875 | Alpha 9847 |
| [1] EI = modulus of elasticity (E) times moment of interia (I). | | |
| [2] As measured by unconfined compression tests | | |
| [2] Protective Jacket Removed from Cable | | |

**Table 2-1. Grout and Cable properties, for TDR composites employed in field monitoring.**

Response of the two cables differed significantly during the ensuing slope deformation.  Between April, 1998 and February, 2000 the thinner, more flexible cable (Cable B) did not respond to deformation, which the thicker, stiffer cable (Cable A) did. Only the results from the 22 mm, solid aluminum outer cable will be employed in subsequent discussions.

Data for the right most TDR cable (Cable A) and slope inclinometer (Inclinometer 1) were collected between installation of the cable (April, 1998) and February 2000.  The TDR responses are shown in Figure 2-2 in the form of the full wave form.  As described in a number of other publications (Dowding, 1994; Dowding, Cole and Pierce, 1999) the reflection signals are reported in terms of millirhos (mρ), which are defined as thousandths of the initial reflected voltage pulse.  The spikes in the signature are

reflections that result from localized shearing of the cable-grout composite.  Extension responses have smaller amplitudes and can be distinguished from those produced by shearing (O'Connor and Dowding, 1996).  The initial spike at the 60 foot depth is a crimp placed in the cable as a reference mark.

The largest responses occurred at depths 92 and 99 feet.  As shown in Figure 2-2, these spikes occur within the zone of highest incremental displacement measured with the slope inclinometer.  Slope inclinometer incremental displacement is defined as the amount of lateral inclination of the inclinometer probe, which corresponds to the slope of the total displacement curve, at each probe position.   A peak in incremental displacement corresponds to a zone of large lateral movement over a small vertical region, which indicates high shear deformation.
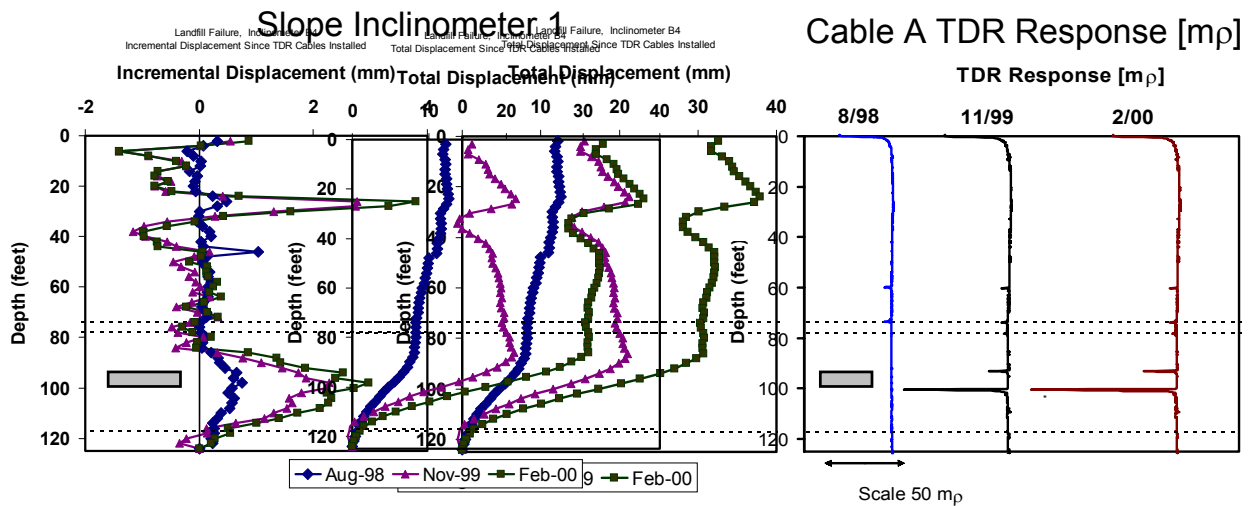


**Figure 2-2.  Slope Inclinometer and TDR Responses from August, 1998 through February, 2000.**

No additional displacement is measured by Inclinometer 2 after August, 1998; however additional displacement is measured by Inclinometer 1 and TDR Cable A,

6

which is shown in Figure 2-2.   The lack of additional displacement measurement by Inclinometer 2 has several possible causes that include: 1) overlying dense fill is failing as blocks that displace relative to each other or 2) Inclinometer 2 was damaged or dislocated during shearing.  Data acquired from the 11 mm cable composite, TDR Cable B, showed no response to the shear displacement measured by the inclinometers. The lack of response can be attributed several possible causes: 1) insensitivity of the cable, 2) the high strength grout ($q_u$ = 4 MPa) used in the installation of TDR Cable B, which prevented sufficient cable deformation to cause TDR voltage spikes, or 3) inadequate soil mass deformation.  The finite element studies in later chapters shed light on the importance of the ratio of grout strength to soil strength.

The results of this field study indicate that TDR cable-grout composites can detect shear displacement of soft soil masses.  However, little is known about the interaction between the soil-mass and the composite during shearing, which limits the design of cable-grout composites for this use.  In succeeding chapters, three dimensional, finite element analysis of the interaction between cable, grout, and soil mass is employed as an approach to designing a cable-grout composite for use in soft soils.

# Chapter 3.  <u>Model Calibration Using Laboratory Shear Test Results</u>

This chapter describes three-dimensional (3D) finite element analysis (FEM) of laboratory shearing of Time Domain Reflectometry (TDR) cables and cable-grout composites to determine appropriate constitutive properties to model interaction of the composite within a soil mass.  In the next chapter these properties will be employed to analyze the three-dimensional interaction of the cable-grout composite with the surrounding soil mass.   This analysis is necessary to determine the most sensitive combination of cable and grout properties for TDR measurement of localized shearing in soft soil under field conditions.

Three different types of laboratory tests were conducted to measure the properties of the cable, grout, and cable-grout composite (Cole, 1999).  The cables themselves were double ring sheared to measure their force-displacement response.  A range of weak cement-bentonite grouts were sheared in unconfined compression to determine their constitutive properties.  Lastly, the cable-grout composites were sheared in a large, three ring shear device to measure the composite transverse force-displacement response, cable-grout interface properties, and the TDR voltage reflection-displacement response.

Required constitutive parameters were determined by matching 3D FEM responses with laboratory measurements described above.  First, an appropriate 3D FE model of cable shearing was developed to backcalculate the cable constitutive properties. These properties were then employed in the cable-grout composite models.  Next the 3D FE model of cable-grout shearing was formulated to determine the appropriate constitutive properties for the grout and interface between the grout and cable.  The

backcalculated model grout strength is compared to the strengths independently determined through unconfined compression.

Finally, a critical shear stress in the cable for initial TDR response was determined from the cable-grout composite model response.  This stress is the calculated cable stress in the cable-grout composite at the minimum deformation for which the laboratory composite produced the first TDR voltage reflection.  This critical stress is necessary to determine the order of magnitude of localized shear deformation required to elicit initial TDR response.  It will be employed in the next chapter for comparison with cable shear stresses calculated with the complete cable-grout-soil composite.

The following discussion will include sections based on: (1) the procedure and results of the cable shear test, (2) finite element modeling of the cable shear test, (3) the procedure and results of the cable-grout composite shear test, (4) finite element modeling of the composite shear test, and (5) back calculation of constitutive properties using the finite element results.

### *Laboratory Cable Shear Test*

#### Apparatus

To determine the shear strength and stiffness of coaxial cables used in Time Domain Reflectometry, an apparatus was devised that would hold a variety of larger diameter coaxial cables (~ 2 centimeter diameter) (Cole, 1999).  As shown in Figure 3-1 and Figure 3-2, the cable shear test apparatus consists of an interior aluminum block approximately five centimeters wide, five centimeters long, and fifteen centimeters deep,

which slides up and down within a larger, split, aluminum block that stabilizes the cable at one end.  The cable is inserted through both blocks, while the holes in both blocks are aligned.  A gap of approximately one millimeter exists between the large, stabilizing block and the smaller, moving block.  The cable is sheared when the internal block is displaced relative to the larger block.  In the field the cable can be controllably sheared (to generate a controlled TDR response to shearing)  by rotating a bolt threaded through the large box into the smaller, mobile box, as shown in Figure 3-3.  In the laboratory, the smaller box is displaced relative to the large stationary box by a piston to acquire the force-displacement response.
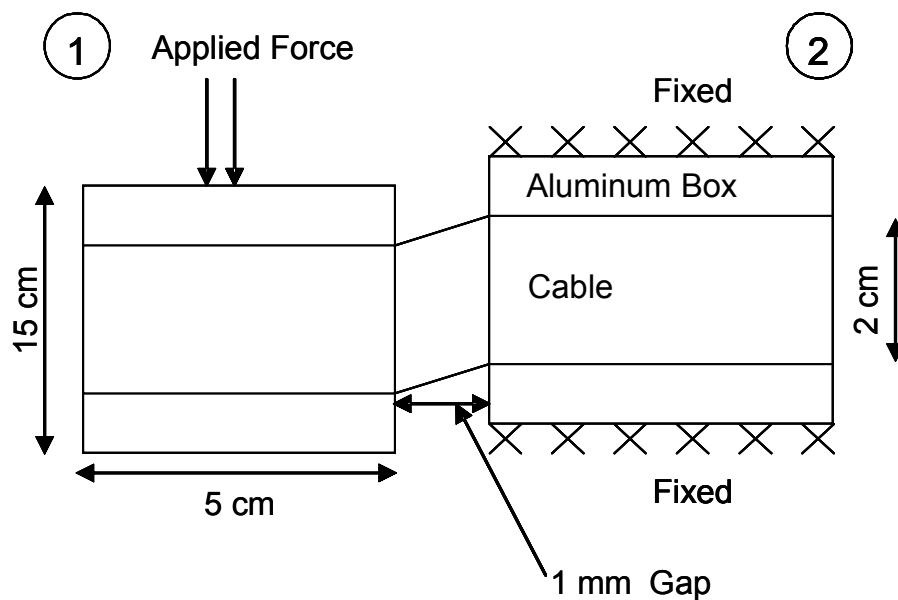


**Figure 3-1. Schematic Drawing of Cable Shear Testing Apparatus.**
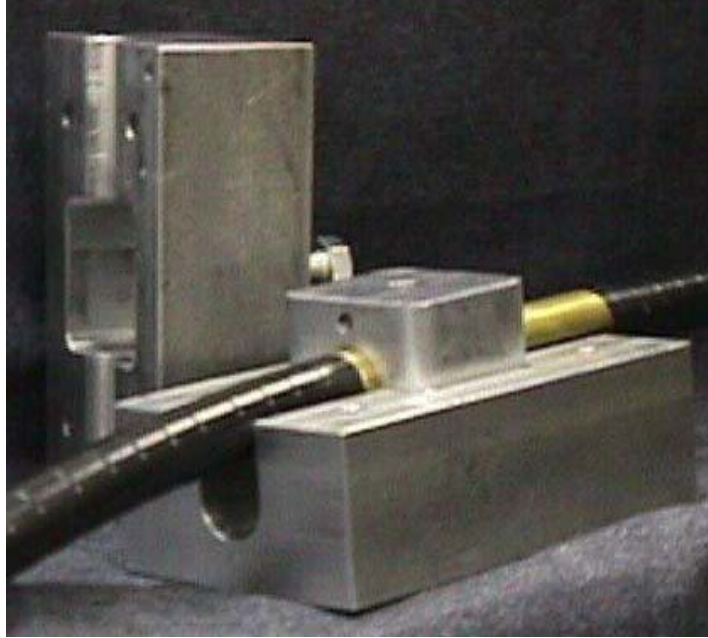
**Figure 3-2. Photograph of Cable Shear Testing Apparatus, the top is removed to show the placement of cable and interior sliding shear block (Cole, 1999).**



**Figure 3-3. Photograph of the assembled apparatus.  The bolt is replaced by a piston for measurement of force-displacement response (Cole, 1999).**

## Cable Types

The shearing device described in the previous section was used to measure the shearing response of a variety of coaxial cables used in Time Domain Reflectometry (Cole, 1999). Although several cables were tested with this device, only two optimum cables and the corresponding test results are modeled in the following finite element analysis. The two cables, shown in Figure 3-4, used in this analysis differ significantly in their construction and deformability: a stiff cable with a solid outside conductor and a compliant cable with a braided outside conductor. The outer radius of both cables is approximately twenty two millimeters (Solid Outer Conductor, r = 22.23 mm; Braided Outer Conductor, r = 21.85 mm).

A commercially available coaxial cable, Commscope Parameter III 875 Cable, commonly used in TDR measurements, provided the base stock for the two alternatives. It is composed of a solid aluminum outer conductor, foam polyethylene dielectric, and a copper-clad, aluminum inner conductor. The solid aluminum outer conductor provides excellent electrodynamic properties for TDR, however it increases the cable stiffness; therefore this cable is optimal for TDR in stiffer media.

The second, coaxial cable is a modified Commscope Parameter III 875 Cable. The outer aluminum conductor has been stripped and replaced with a tin/copper braid and PVC, shrink-wrapped, sheathing. The braided outer conductor results in a more compliant cable and provides adequate electrodynamic properties. Throughout this report the cables will be referred to as "solid cable" and "braided cable", which refers to the outer conductor.
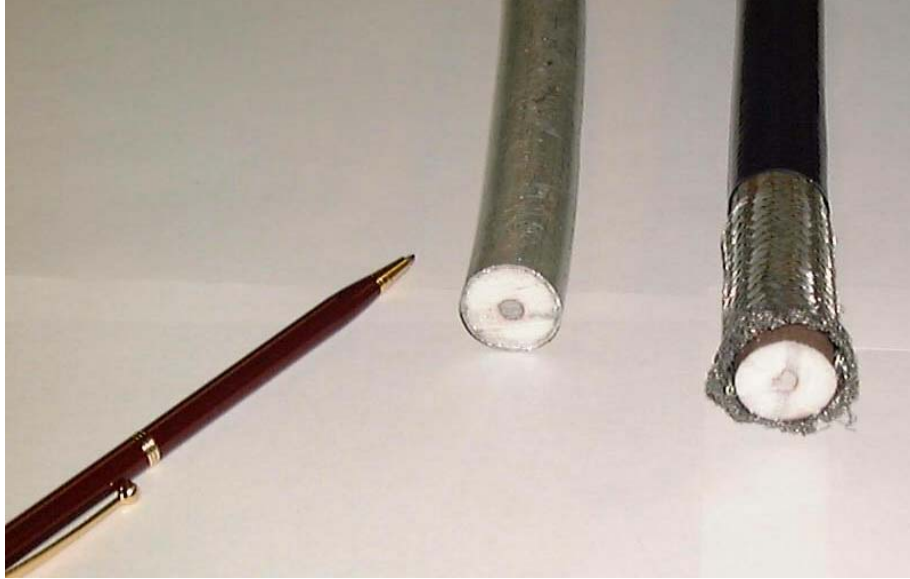
**Figure 3-4. Different cables tested using the Cable Shear Box apparatus. Solid aluminum outer conductor cable is on left, braided tin/copper outer conductor cable is on right.**

## Laboratory Test Results

Results from the cable shear tests are given in the form of vertical force-versus-vertical (shear) displacement plots for different cable types (Cole, 1999). The physical properties that can be determined from the force-displacement plots include cable stiffness and cable strength. Figure 3-5 gives the results from the previous laboratory testing. By matching these force-displacement curves with the results from three dimensional finite element simulations, appropriate values of constitutive parameters can be determined for these cable types.
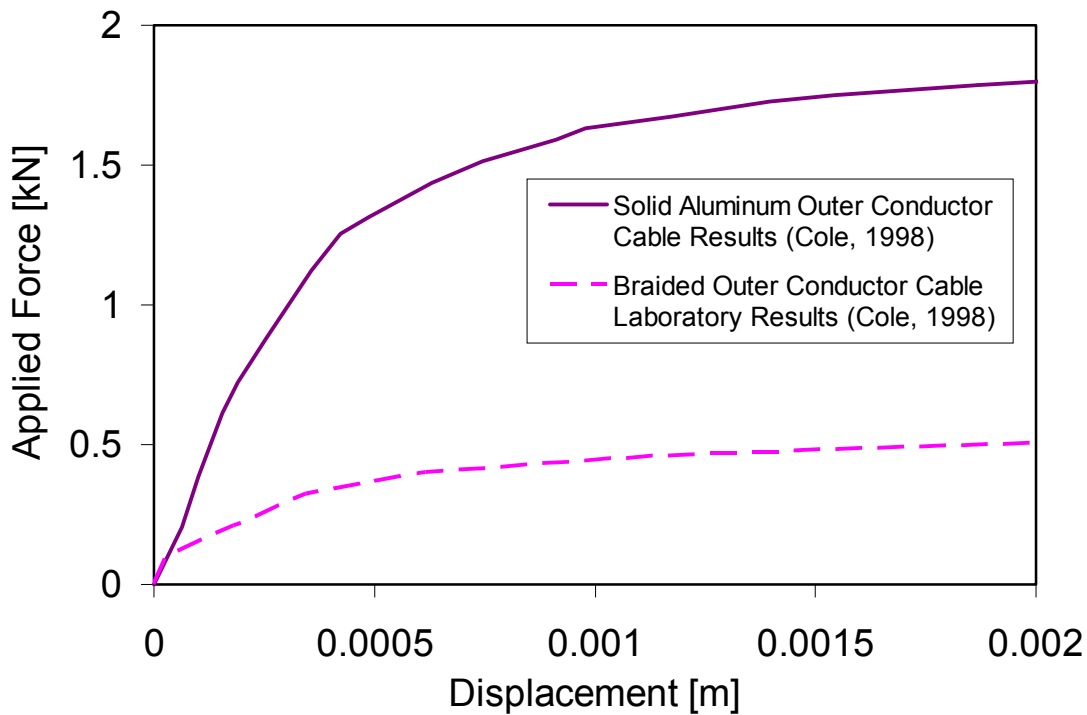
**Figure 3-5. Force-Displacement Curves from laboratory shearing of coaxial cables (Cole, 1999).**

## *Finite Element Analysis of Cable Shear Test*

### Plaxis 3D Tunnel

A commercial three-dimensional finite element package, Plaxis 3-D Tunnel, is used to model the behavior of two coaxial cables during the shearing test discussed above. Plaxis 3D Tunnel is a special purpose three-dimensional finite element software package designed for various tunnel applications in soil and rock. Similarity in geometry of a cable and a tunnel allows for finite element analysis of Time Domain Reflectometry cable-grout composites in soil.

The three-dimensional automatic mesh generation procedure in Plaxis allows for local refinement and generation of the mesh, in three dimensions, relative ease. The input procedure begins with creating the geometry of a two-dimensional cross-section (slice) of the model, which is formed into a two-dimensional mesh consisting of six-noded triangular elements, as highlighted in Figure 3-6. From this cross-section the three dimensional mesh is produced by extruding the two-dimensional 'slices', in the axial direction, with different thicknesses. The thicknesses of the compiled slices are restricted by Plaxis, according to the coarseness of the two-dimensional mesh to avoid computationally unstable, thin elements. A nominal thickness limit of ten times the smallest element width is used by Plaxis. The material element properties can be assigned in each individual slice, modeling the different soil and cable properties in the radial and axial directions. Similarly, prescribed displacements and tractions can be assigned to selected nodes in each slice.

The three-dimensional mesh consists of fifteen-noded, triangular prism ('wedge') material elements and eight-noded, 'zero-thickness', interface elements. The highlighted element in the corner of the first slice in Figure 3-6 illustrates a typical wedge element. Nodes are located at each of the six corners and at the nine midpoints of the edges. Interface elements have no thickness, but have shear stiffness and strength properties that can be specified separately from the material elements. The interface elements will be discussed in more detail in the next chapter.

Plaxis 3D Tunnel offers a variety of material models. The Mohr-Coulomb material model is used for all elements, which employs a linearly elastic-perfectly plastic stress-strain response. The Mohr-Coulomb material model does not account

automatically for initial consolidation properties or time effects.  However, the Mohr-Coulomb material model does allow plastic deformation once the material element has met the Mohr-Coulomb failure criteria.  The effects of the non-linearities will be evident in the resultant force-displacement curves, shown later.
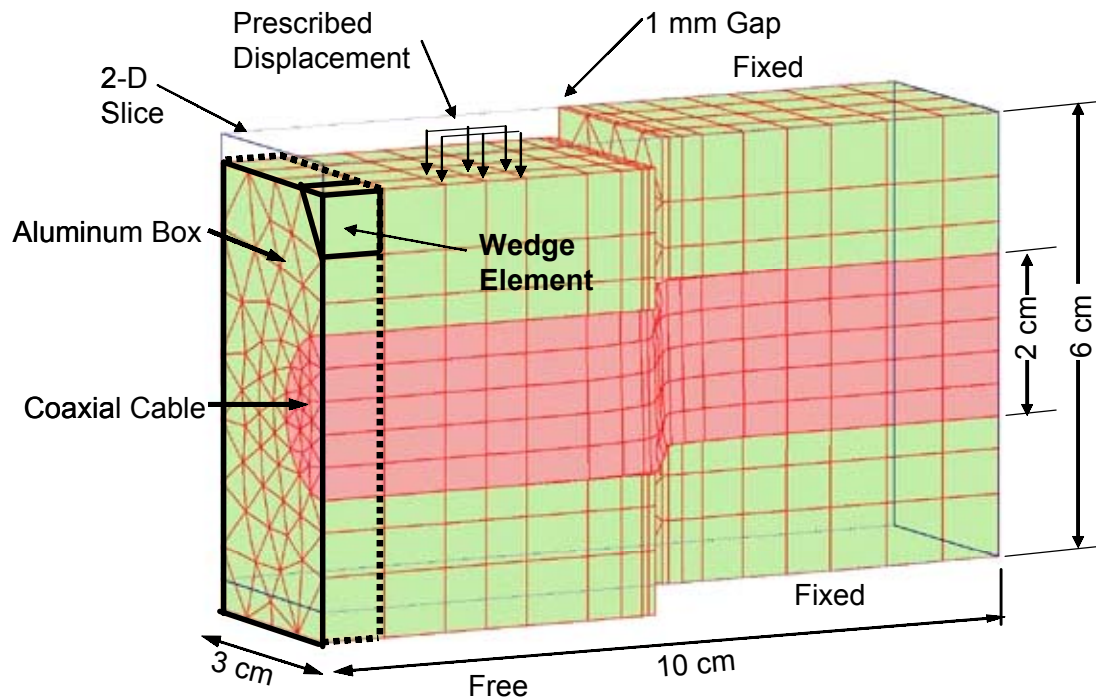


**Figure 3-6.  Three Dimensional Output Mesh, Showing Vertical Shearing of Coaxial Cable Model.  Also highlighted is an individual wedge element and two-dimensional slice.**

## Model Geometry

As shown in Figure 3-6, generated model geometry consists of right and left blocks with the material properties of aluminum, separated by one millimeter; the coaxial cable, modeled as one continuous unit, passes through each aluminum block. The right aluminum section is fixed in the vertical direction, whereas the left aluminum section has a prescribed displacement in the vertical direction at the location corresponding to the

piston in the laboratory model. The model geometry only consists of half of the laboratory shear test apparatus due to model symmetry. Presentation of this split model enables observation of cable behavior inside the aluminum apparatus.

## Material Parameters

The Mohr-Coulomb material parameters that are variable in this analysis are the modulus of elasticity (E) and the cohesion (c) of the coaxial cable. Parameters that remain constant are the Poisson's ratio ($\nu$) and friction angle ($\phi$); additional parametric studies show that $\nu$ and $\phi$ have relatively small effects on the resultant curves (See Appendix A for discussion). The interface strength and stiffness between the aluminum blocks and coaxial cable is held constant, with an shear modulus of 90,000 kPa and cohesion of 1,400 kPa. Its value is of little importance in subsequent analyses because this interface does not the interface properties between the coaxial cable and grout. The interface properties describing the interface between the grout and cable used in TDR is discussed in the section on composite shear testing.

The aluminum blocks are assigned material properties that represent actual aluminum; however, as long as the aluminum blocks have a considerably higher modulus of elasticity and strength than the cables, the material properties of the blocks are insignificant. For instance, the modulus of elasticity for aluminum is 70,000,000 kPa versus 75,000 kPa for the solid cable.

## Cable Model Results

Material parameters for both the solid cable and the braided cable are estimated by adjusting the cable's constitutive properties until the computed finite element force-displacement response fits the measured response during laboratory shearing. The

17

deformed finite element mesh in Figure 3-6 shows the relative displacement and shearing of the cable inside the aluminum blocks.  Figure 3-7 compares the best fit calculated response for the solid cable and braided cable with that measured. The finite element model responses lack the gradual curvature seen in the laboratory results in part because of the linear elastic-perfectly plastic characteristics of the Mohr-Coulomb material and interface models.  The modulus of elasticity and cohesion (strength) properties of the cable are determined by matching the average measured elastic and ultimate strength responses.

Values of material parameters corresponding to the best fit curves are listed in Table 3-1.  These parameters are used in the finite element models of cable-grout composites described in the next section, which incorporate interaction between the coaxial cable and surrounding grout.
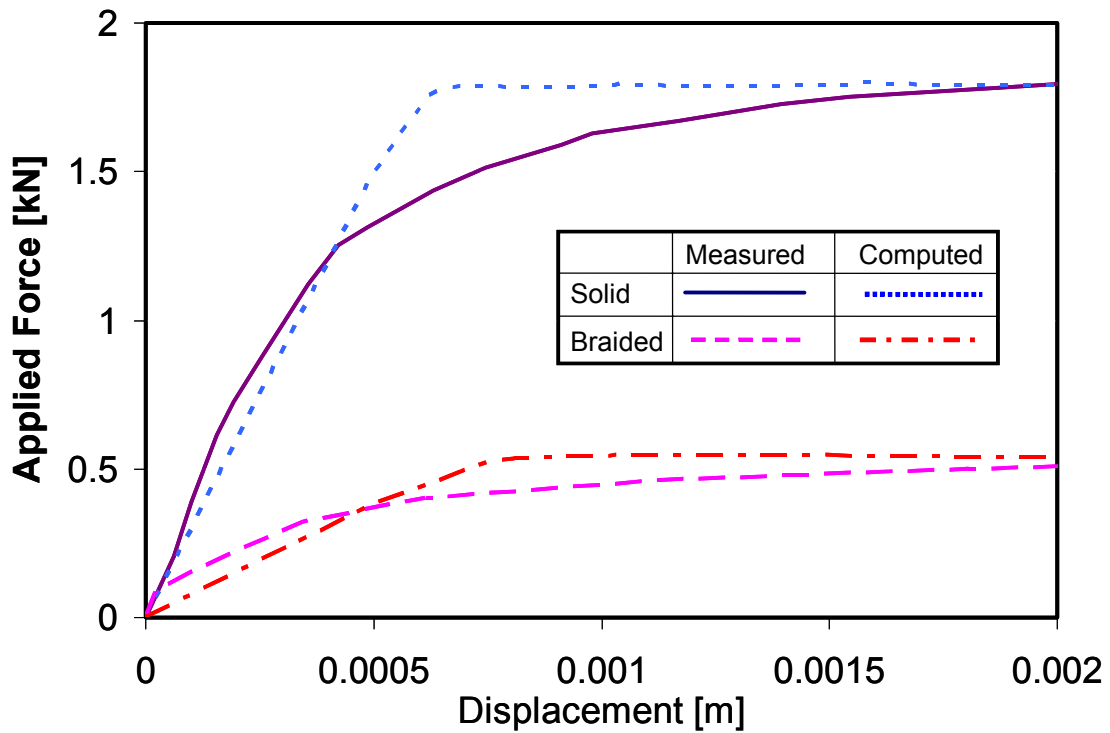
**Figure 3-7. Comparison of Finite Element Analysis Results with Laboratory Cable Shear Test Response (Cole, 1999) for Solid Aluminum Outer Conductor Cable and Braided Outer Conductor.**

| Cable Parameter Results | | | |
|---|---|---|---|
| **Parameter** | **Symbol** | **Values** | |
| | | **Solid Aluminum Outer Conductor** | **Braided Outer Conductor** |
| **Modulus of Elasticity** | E | 300,000 kPa | 75,000 kPa |
| **Cohesion** | c | 4,700 kPa | 1,400 kPa |
| **Unconfined Compressive Strength** | $q_u$ | 9,400 kPa | 2,800 kPa |
| **Friction Angle** | $\phi$ | 0° | 0° |
| **Poisson's Ratio** | $\nu$ | 0.2 | 0.2 |

**Table 3-1.  Parameter values obtained through back-calculation procedure.**

## *Laboratory Cable-Grout Composite Shear Test*

**Apparatus**

      Shear response of various coaxial cable-grout composites have been measured by shearing a three-part cylinder with a modified controlled displacement loading device (Cole, 1999). As shown in Figure 3-8 and Figure 3-9, the end sections of the cable-grout composite cylinder are placed in saddles to brace the cylinder while the center section is displaced downward. The downward displacing piston is fitted with a curved steel frame, to distribute the load across the center cylinder section. Dial gauges monitor vertical (shear) displacement of the center section, relative to the ends; similarly a proving ring monitors vertical force required to displace the center section.
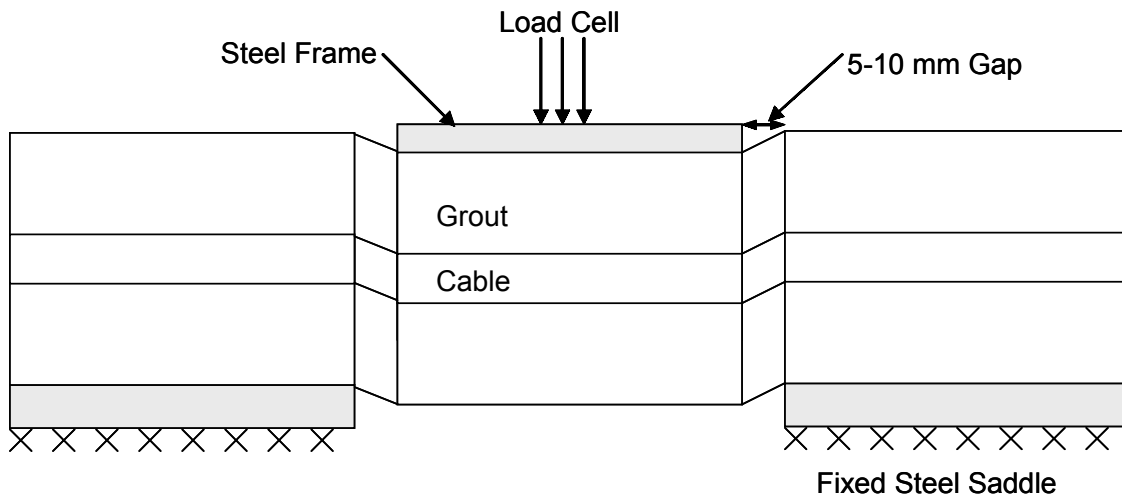
**Figure 3-8. Schematic of Grout-Coaxial Cable Shear Testing Apparatus.**
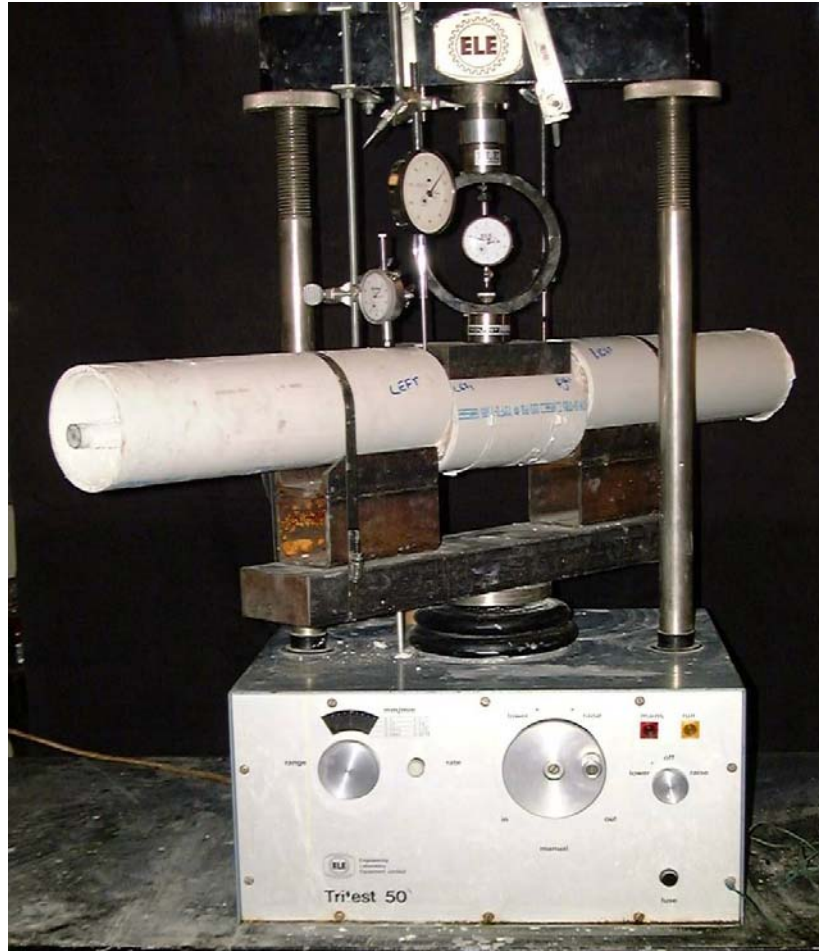
**Figure 3-9. Photograph of Actual Composite Shear Test Apparatus.**

The composite cylinders are approximately ten centimeters in diameter, with the two centimeter diameter coaxial cable grouted into the center of the cylinder. Gaps between the saddles, which brace the end sections of the cylinder, and the loading frame, which displaces the center section of the cylinder, are between five and ten millimeters. The open ends of the composite cylinder allow for TDR signals to be transmitted and recorded.

Also recorded during the shearing was the TDR signal reflection amplitude versus relative displacement. These reflection-displacement relations were employed to

determine the minimum deformation at the interface necessary to produce a measurable

reflection. This approach was employed to measure the load-deformation response of

composites from a wide variety of different cable types and grout strengths (Cole, 1999).

**Laboratory Test Results**

The composite shear test results for both solid and braided cables are shown in the

form of a vertical force versus vertical displacement relation, in Figure 3-10, and TDR

signal reflection amplitude versus displacement relation, in Figure 3-11.  These responses

are for cable-grout composites with the most compliant grout that is stiff enough to

produce a TDR voltage reflection.  Constitutive properties for the grout had been

independently measured by results of unconfined compression testing(Cole, 1999).
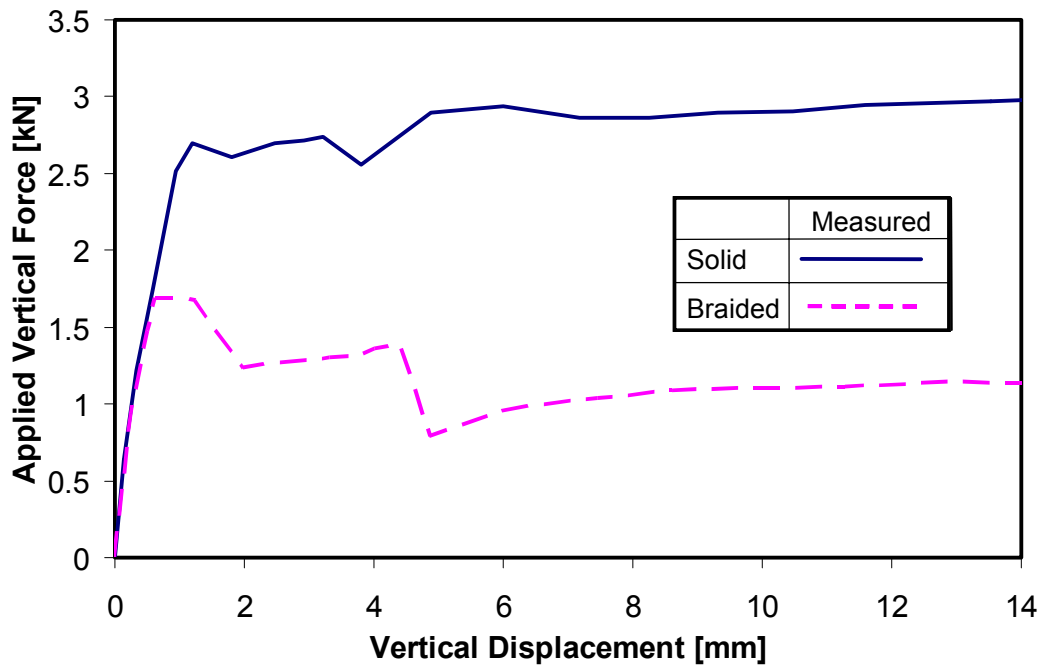


**Figure 3-10. Laboratory Composite Shear Test Results (Cole, 1999).**

**Time Domain Reflectometry Voltage Reflection vs. Shear Displacement**
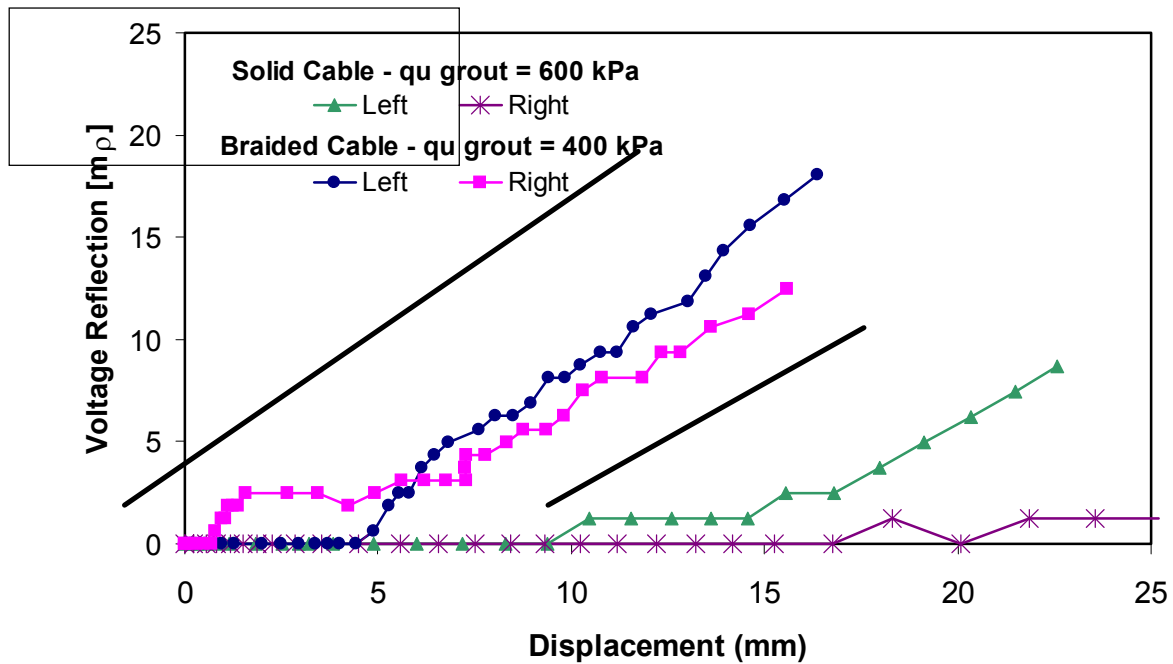


**Figure 3-11. TDR Reflection versus Shear Displacement for shearing of cable-grout composite with 400 kPa and 600 kPa strength grouts. (Cole, 1999).**

Separation between the grout and cable, after loading, shown in Figure 3-12, provides information necessary to determine the interface strength between the two materials. During loading the cable will indent into the grout in one direction and separate from the grout in the opposite direction. This separation is modeled with special interface elements in Plaxis, which is discussed in a later section, describing the results of the FE simulation.

Separation between Grout and Cable
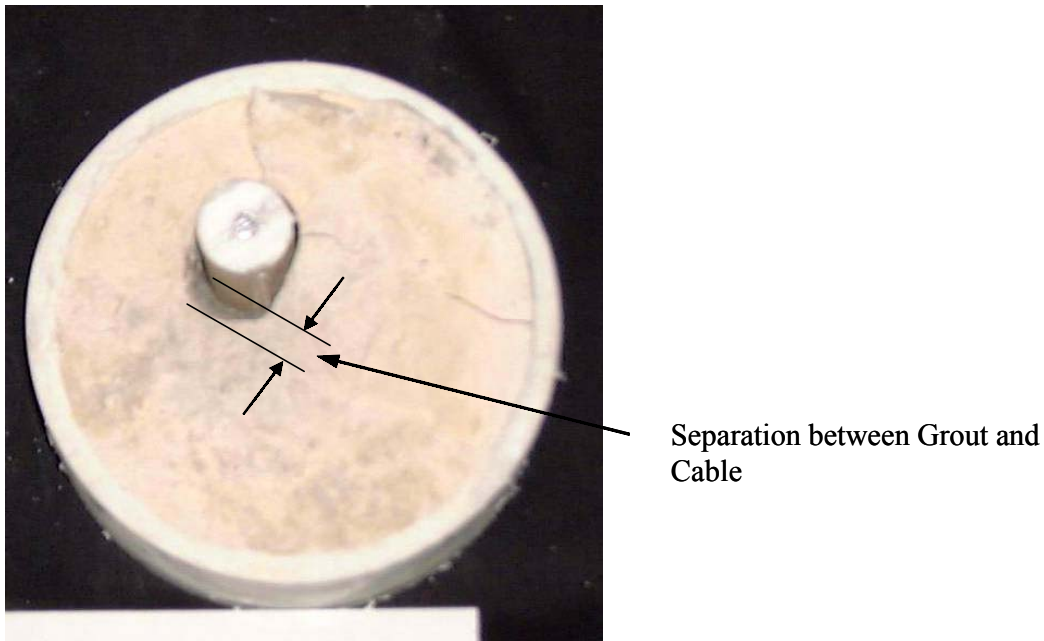
**Figure 3-12. Example of Separation Between Cable and Grout After Shearing (Cole, 1999).**

The minimum cable deformation (or shear stress) required to generate a TDR response is an important parameter to determine through finite element modeling. This critical parameter can be determined by modeling the laboratory results for TDR reflection versus vertical displacement of the composite shown in Figure 3-11. The responses are for solid and braided cables embedded in 600 kPa grout and 400 kPa grout, respectively. There are two lines shown for each cable type in Figure 3-11, corresponding to the right and left shear zones in the laboratory apparatus. The minimum relative displacement necessary for TDR reflection for cables is determined from the results shown in Figure 3-11. The minimum relative displacement for both the solid cable and the braided cable is difficult to evaluate. The TDR reflection is apparent after one millimeter of relative displacement for the right shear zone of braided cable, yet is apparent after four millimeters of relative displacement for the left shear zone of braided

cable. The discrepancy in displacements and the immediate TDR reflection is probably

the result of rotation of the center section. Therefore the minimum relative displacement

is determined by drawing a 'best fit' line through the sloping TDR response lines, using

the x-axis intercept as the minimum relative displacement. A similar approach is used for

the solid aluminum cable results to determine the minimum relative displacement of the

composite.

Cable shear stress, or cable deformation (slope), calculated with the 3-D model at

the minimum "measured" relative displacement can be employed as a criterion for

modeling the interaction of TDR composites and surrounding soil in subsequent analyses.

By displacing the cylinder section of the cable-grout composite in the finite element

model an amount equal to the laboratory test displacement, the associated shear stress

levels in the cable are calculated, as discussed in the finite element analysis section.

## *Finite Element Analysis of Grout-Cable Composite Shear Test*

### Model Geometry

Plaxis 3-D Tunnel was used to create and execute a finite element analysis of the

composite shear test described previously. Instead of modeling the apparatus as two end

sections and a displaced middle section only two sections were used: a fixed end section

and the displaced middle section. Figure 3-13 shows the three-dimensional mesh

generated for the composite. As with the cable shear model, symmetry allowed for

calculation with only one axial half of the composite and shear apparatus.
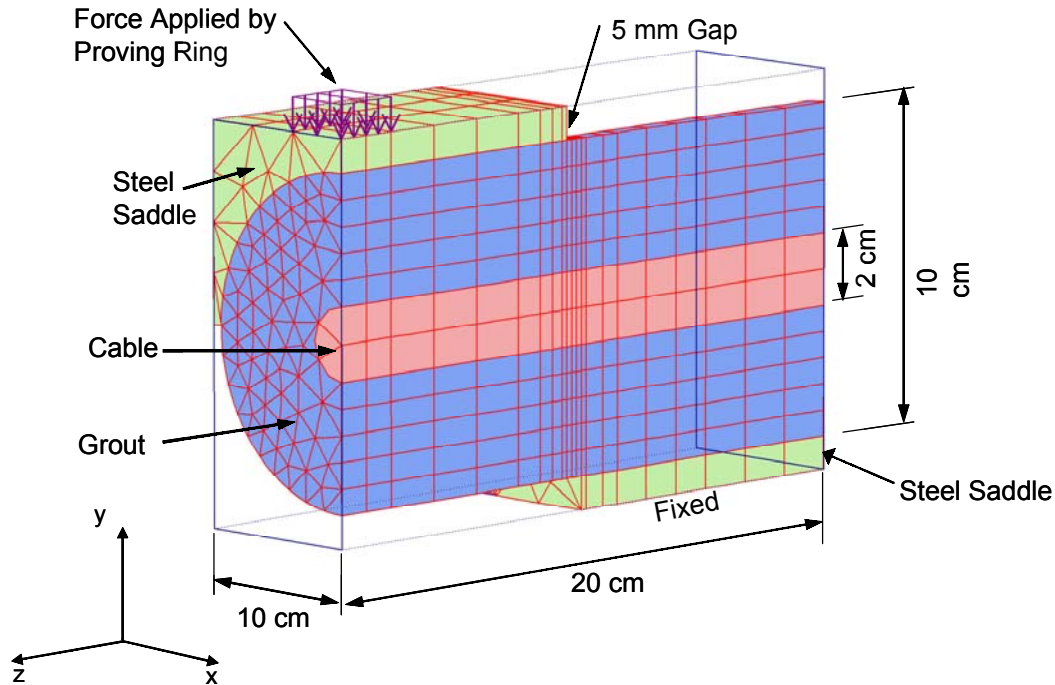
**Figure 3-13. Three Dimensional Mesh, showing cable, surrounding grout, and shear apparatus (saddles).**

The left cylinder section (center section in Figure 3-8 and Figure 3-9) is assigned a prescribed displacement at the point of contact between the proving ring and the steel frame.   As discussed in the previous finite element section, all material models are based on the Mohr-Coulomb failure criteria.  Interface elements separate the cable and grout, to allow relative movement between the grout and cable.  Interface strength between the external restraint and the grout is not tracked as the TDR composite will be placed in rock or soil and thus the interface properties will differ greatly in the ultimate model.

The finite element model is operated several times, with different goals: (1) the model is displaced enough to match the laboratory measured force-displacement curves and (2) the model is displaced the minimum measured relative displacement needed to generate a TDR response in the laboratory tests.  The second displacement is undertaken

to analyze cable deformation and shear stresses generated in the cable at the time of the first TDR reflection.

**Finite Element Analysis of Composite Shearing Results**

Grout strength and stiffness parameters are found by matching calculated response of solid aluminum and braided cables with force-displacement curves measured in the laboratory, as shown in Figure 3-14. The interface strength parameter between the grout and cable is found by simultaneously matching the calculated and measured force-displacement curves, while observing similar calculated and measured separation between the grout and cable. The best fit calculated force-displacement curves are compared to the laboratory curves in Figure 3-14. Because the material models are based on Mohr-Coulomb failure criteria, it is not possible to model the post-failure softening of the Braided Cable response. However, the initial stiffness and yield point of the laboratory results are faithfully reproduced. The model material parameters that were employed to match the measured laboratory results are listed in Table 3-2. Table 3-3 compares the calculated and measured grout unconfined compression strengths and cable-grout separation.

| Grout-Coaxial Cable Model Test Results | | |
|---|---|---|
| | Solid Aluminum Outer Conductor Cable | Braided Outer Conductor Cable |
| Unconfined Compression Grout Strength (Model Results), [kPa] | 700 | 450 |
| Grout Modulus of Elasticity (model results) [kPa] | 75,000 | 75,000 |
| Shear Stress in Cable for Initial TDR Response [kPa] | 2000 | 350 |
| Slope of Cable for TDR Response | 0.13 | 0.065 |
| Interface Cohesion [kPa] | 90 | 30 |
| Interface Shear Modulus (G) [kPa] | 50 | 13 |

**Table 3-2. Backcalculated parameters obtained by finite element modeling of the composite shear test.**

| Grout-Coaxial Cable Composite Shear Test Results | | | | |
|---|---|---|---|---|
| | Grout Strength, $q_u$, [kPa] | | Grout/Cable Separation [mm] | |
| | Measured (Unconfined Compression Test) | Acquired by Model Calibration | Measured Composite Shearing Test | Calculated FE Analysis |
| Solid Aluminum Outer Conductor Cable | 600 | 700 | 12.3 | 5.8 |
| Braided Outer Conductor Cable | 400 | 450 | 5.3 | 2.2 |

**Table 3-3. Comparison of Measured and Calculation Unconfined Compression Strength and Grout-Cable Separation (Cole, 1999).**

Interface parameters, describing the strength and stiffness of the interface between the grout and coaxial cable, are also calibrated by matching the calculated and measured force-displacement curves as shown in Figure 3-14. Calculated and observed separations between the grout and cable during relative displacement are shown in Figure 3-15. The

parameters that are calibrated to provide a match between the calculated and observed force-displacement responses are the shear modulus of the interface elements, $G_{inter}$, and the cohesion of the interface elements, $c_{inter}$. Also observed during the analysis was a similar separation between grout and cable for both the calculated and observed composite responses. The interface shear modulus affects the 'slip' and the 'separation' between the grout and cable materials during relative displacement. Because the materials used in the finite element model are assigned zero friction angles, the shear strength of the interface elements is equal to their cohesion. Plaxis 3D Tunnel employs a multiplier coefficient $R_{inter}$ to assign the strength and stiffness of the interface elements. The cohesion of the interface element is assigned as a fraction of the cohesion of the cable cohesion, therefore the interface cohesion is equal to $R_{inter}$ times the cable cohesion ($c_{inter} = R_{inter}*c_{cable}$). Similarly, the shear modulus of the interface elements ($G_{inter}$) are equal to the shear modulus of the cable ($G_{cable}$) times $R_{inter}$ squared ($G_{inter} = (R_{inter}^2) *$ $G_{cable}$). Figure 3-16 shows the sensitivity of the calculated force-displacement responses to the variation of the interface parameter $R_{inter}$.

In addition to calibrating the grout strength and interface parameters, the finite element model provides information regarding the change in cable geometry and shear stresses produced in the cable during relative displacement between the left and right sections. Calculated shear stress acts in the vertical direction on the plane normal to the axial direction ($\sigma_{yz}$, with axes shown in Figure 3-13). Figure 3-17 shows these shear stresses ($\sigma_{yz}$) in the cable following displacement. The value of shear stress reported in Table 3-2 is that calculated in the cable at minimum relative displacement necessary to generate the first TDR response as reported in the Laboratory Results section.

Cable deformation after relative displacement between the left and right sections, shown in Figure 3-18, can also be used as a TDR response criterion. The deformations can be employed to compute its slope; the slope reflects the change in cable geometry due to relative displacement between the left and right cylinders. The calculated critical cable shear stress and cable slope provides criteria for the minimum shear stress or slope needed to generate a TDR response from localized shearing. These criteria are necessary for interpreting finite element models of soil-grout-cable interactions in the next chapter.
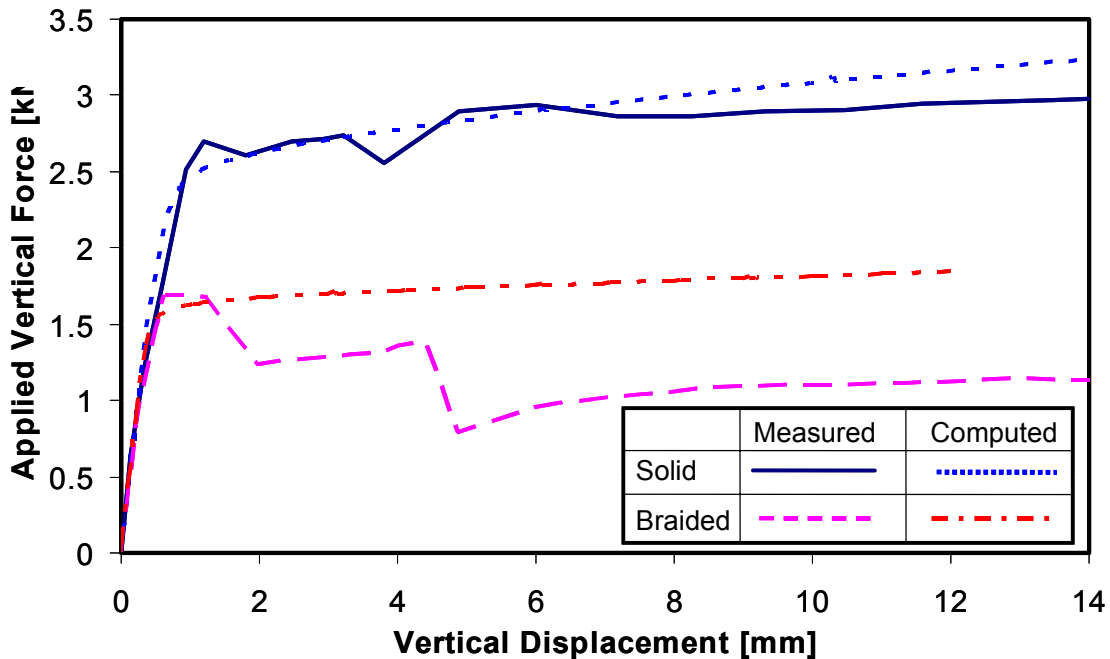


**Figure 3-14. Comparison of Model Force-Displacement Curves and Laboratory Curves.**

Separation between Grout and Cable after Displacement
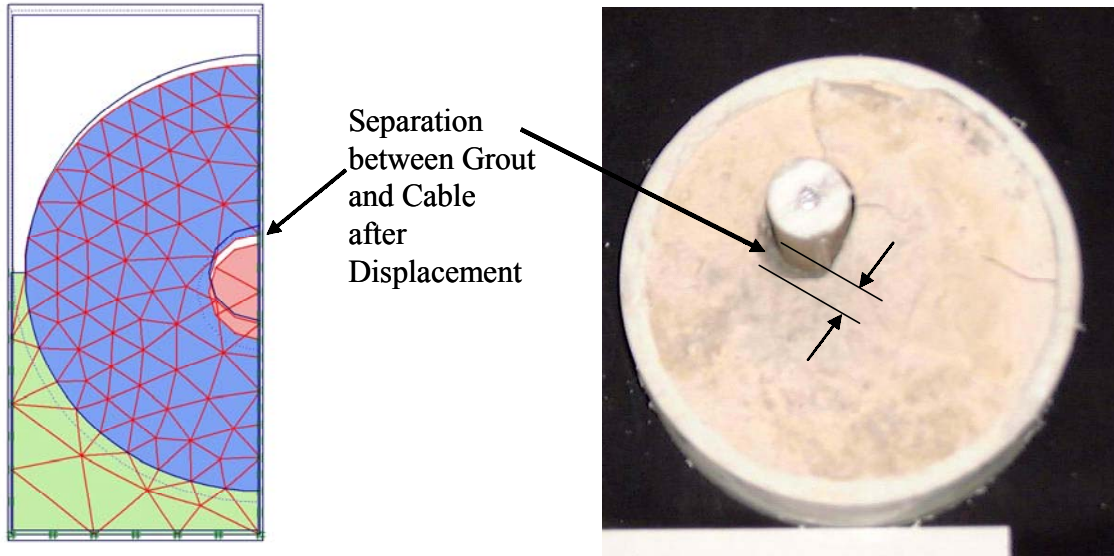
**Figure 3-15. Comparison of measured and calculated grout-cable separation.**



|  |  |  | $q_u$ [kPa] | E [Mpa] | R |
|---|---|---|---|---|---|
| Measured |  | | 660 | - | - |
| Calculated |  | |  |  |  |
|  |  | 1 | 700 | 75 | 0.01 |
|  |  | 2 | 700 | 75 | 0.02 |
|  |  | 3 | 700 | 75 | 0.03 |
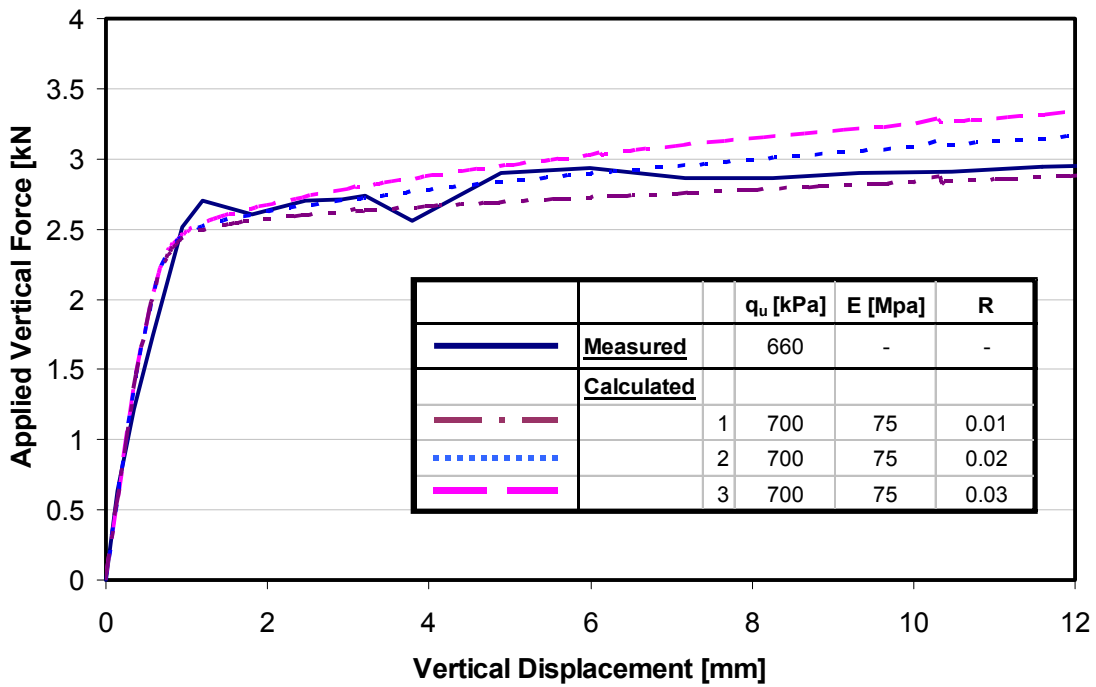
**Figure 3-16. Sensitivity of force-displacement results to variation in constitutive parameter for the interface between the cable and grout for solid aluminum outer conductor cable.**
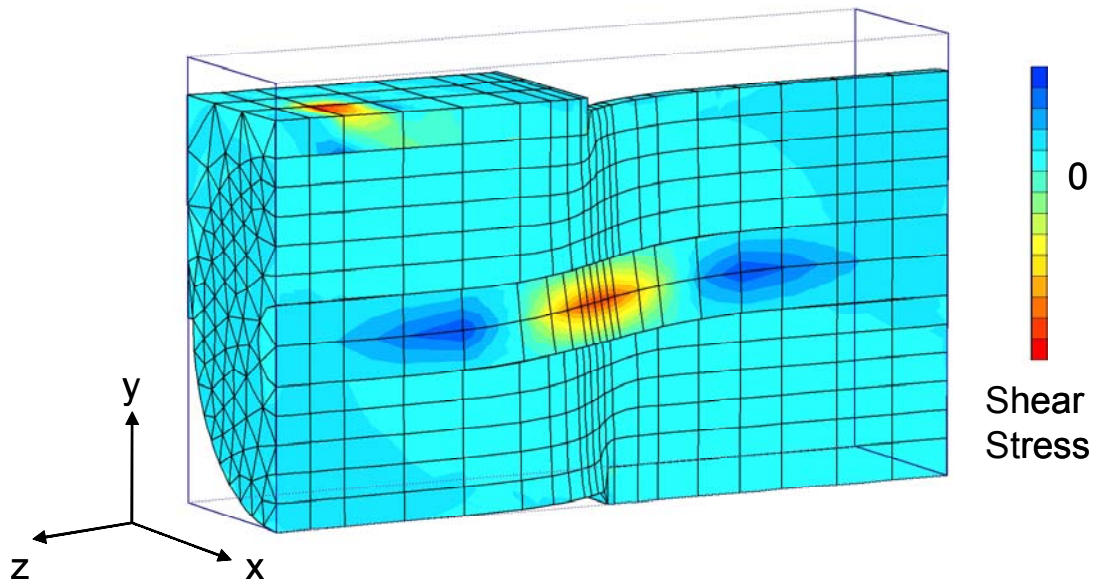
**Figure 3-17.  Shear Stress ($\sigma_{yz}$) acting in y-direction, on plane perpendicular to z-direction in Coaxial Cable. Produced by a displacement of 15 mm relative to the fixed right hand section.**
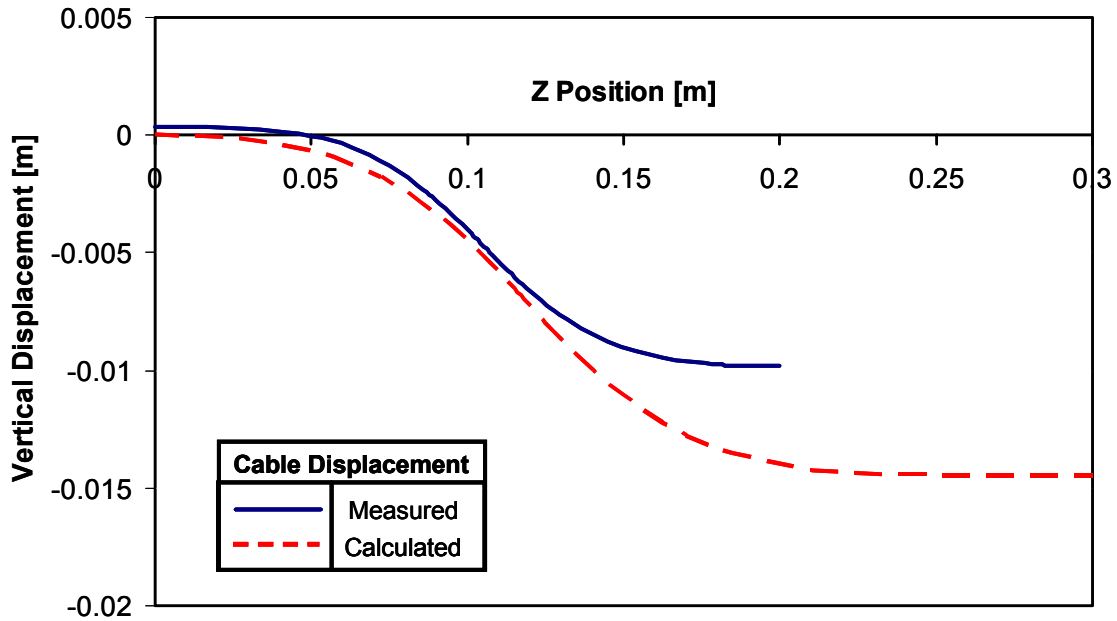
**Figure 3-18. Cable deformation for laboratory model example and soil-composite interaction model example.**

## *Summary*

Three-dimensional finite element analyses of laboratory shearing of: 1) TDR cable and 2) TDR cable-grout composites have resulted in parameter calibration for a range of coaxial cables and grout types. The parameter calibration occurred in three steps. First, values of cable strength and stiffness were acquired by matching measured force-displacement responses with finite element model responses of cables sheared in the laboratory. Second, values of grout strength and stiffness, as well as the interface strength between the grout and cable, were acquired by matching measured force-displacement responses with finite element model responses of the cable-grout composites sheared in the laboratory, while also calculating separation between the grout and cable. Thirdly, shear stresses within the cable and deformation (slope) of the cable

associated with first TDR voltage reflections were calculated for two cable-grout

composites with the model parameters determined in the first two steps. These critical

shear stress and cable slope values will be used as response criteria for models of the

interaction of TDR cable-grout composites in different soils, for which there are no

laboratory measurements for calibration.

Table 3-4 provides the material parameters and critical values calculated in this

chapter. The coaxial cable and interface parameters calculated will remain constant

throughout models of TDR cable-grout composites in different soil types. The

calculated grout parameters independently verify the finite element model of the

composite, by showing the similarity between the grout strengths as back-calculated with

the model and those measured in unconfined compression. The critical cable shear stress

and critical cable deformation (slope) will be used in future soil-composite models to

provide numerical criteria necessary to interpret model results.

| Model Calibration Results - Physical Parameters | | | | | |
|---|---|---|---|---|---|
| | | Symbol | Solid Aluminum Outer Conductor | Braided Outer Conductor |
| Cable Shearing Results | Cable Strength [1] [kPa] | $c_{cable}$ | 4,700 kPa | 1,400 kPa |
| | Cable Modulus of Elasticity [1] [kPa] | $E_{cable}$ | 300,000 kPa | 75,000 kPa |
| Grout and Interface Parameters | Grout Strength [1] [kPa] | $c_{grout}$ | 350 kPa | 225 kPa |
| | Grout Modulus of Elasticity [1] [kPa] | $E_{grout}$ | 75,000 kPa | 75,000 kPa |
| | Interface Strength [1] [kPa] | $c_{interface}$ | 90 kPa | 28 kPa |
| | Interface Shear Modulus [1] [kPa] | $G_{interface}$ | 50 kPa | 13 kPa |
| Critical Cable Response | Critical Cable Shear Stress [kPa] | $\sigma_{yz}$ [2] | 2000 kPa | 350 kPa |
| | Critical Cable Slope | $\gamma_{yz}$ [2] | 0.13 | 0.065 |
| [1] $c = (1/2)*q_u$, $\nu=0.2$, $\phi=0°$ | | | | |
| [2] Using Axes shown in Figure 3-1, and standard mechanics notation. | | | | |

**Table 3-4. Calibrated Model Parameters and Calculated Critical Values.**

# Chapter 4.  <u>Finite Element Analysis of Soil-Grout-Cable Interaction in Time Domain Reflectometry</u>

Measurement of localized shear displacement in soft soil with Time Domain Reflectometry (TDR) cables requires use of an optimum combination of cable and grout properties for a given soil condition.  In this chapter three-dimensional (3D) finite element (FEM) analyses of the interaction of cable-grout composites with the surrounding soil are employed to determine the optimum combination.  Cable, grout and cable-grout interface properties employed in these analyses were determined by direct measurement as well as comparison of calculated 3D FEM and measured laboratory shearing responses of cable-grout composites.  The critical property that allows the extrapolation of laboratory to field response is minimum shear stress in the cable, or maximum curvature of the cable, associated with the first TDR reflection.  Details of these property determinations were described in the previous chapter.

Optimum cable design is constrained by two dominant failure mechanisms: 1) grout that is too weak (compliant) to shear the cable sufficiently to produce a signal reflection and 2) a cable-grout composite that is too strong (stiff) and causes the soil mass to shear around, rather than through, the composite (and cable).  By analyzing a variety of cable, grout, and soil combinations, the appropriate cable can be paired with an optimally stiff grout to produce the critical shearing stress in the cable.  This optimum design provides a grout with enough strength (stiffness) to adequately deform the cable, yet is weak (compliant) enough so as to limit failure in the surrounding soil mass.

The FEM analyses of the interaction between the cable-grout composite and surrounding soil is described in the following sections: 1) development of model geometry and loading, 2) assignment of material parameters, 3) model operation with incrementally changed grout properties, 4) comparison of results to critical shear stress levels, determined in the previous chapter, and 5) discussion of optimal grout and cable selection based on FEM results and comparisons.

## *Finite Element Model Geometry*

### Geometry and Loading

The commercially available finite element analysis program Plaxis 3-D Tunnel, as described in the previous chapter, was used for analyzing the cable-grout-soil interactions. The process for defining an initial geometry begins with creating a two-dimensional slice, like that shown in Figure 4-1, which is then extended to three dimensions by adding slices perpendicular to the plane of this view. The resulting 3D model is shown in Figure 4-2. Although the interface elements have zero thickness they are graphically expanded to be visible. The small gaps without material elements adjacent to the cable-grout interface and grout-soil interface are a graphical representation of the two nodes at the interface, which correspond to the interface elements.
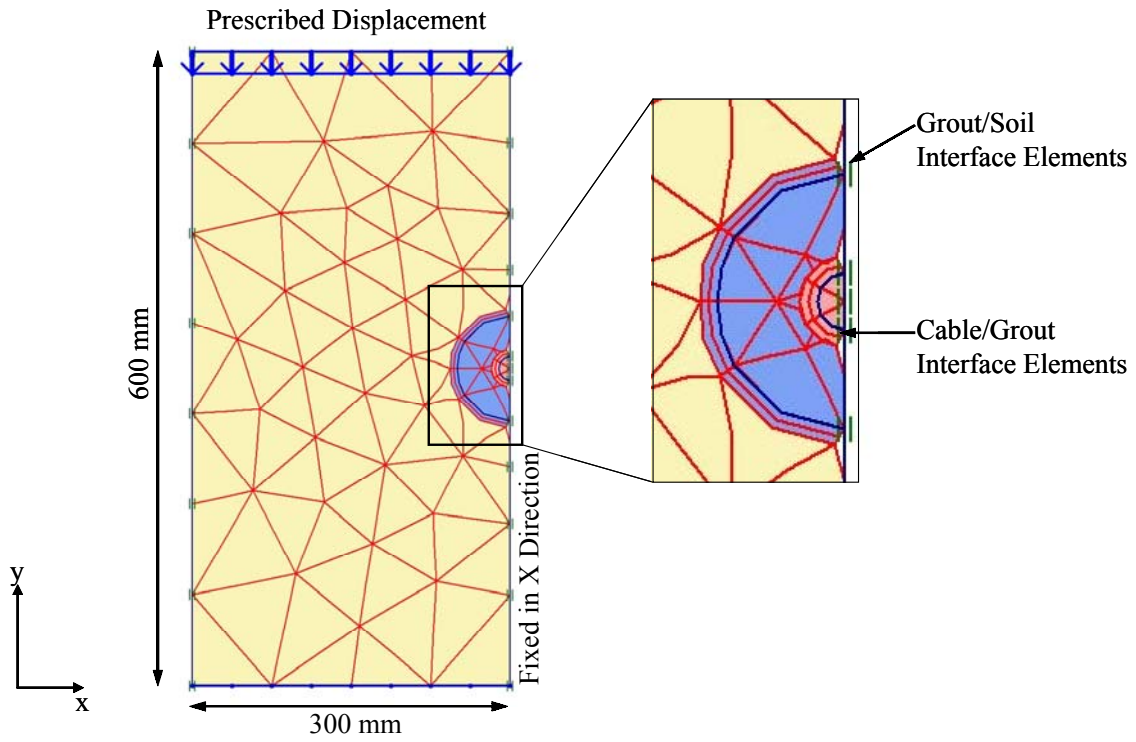
**Figure 4-1. Two Dimensional View of Geometry Used in Finite Element Model.**
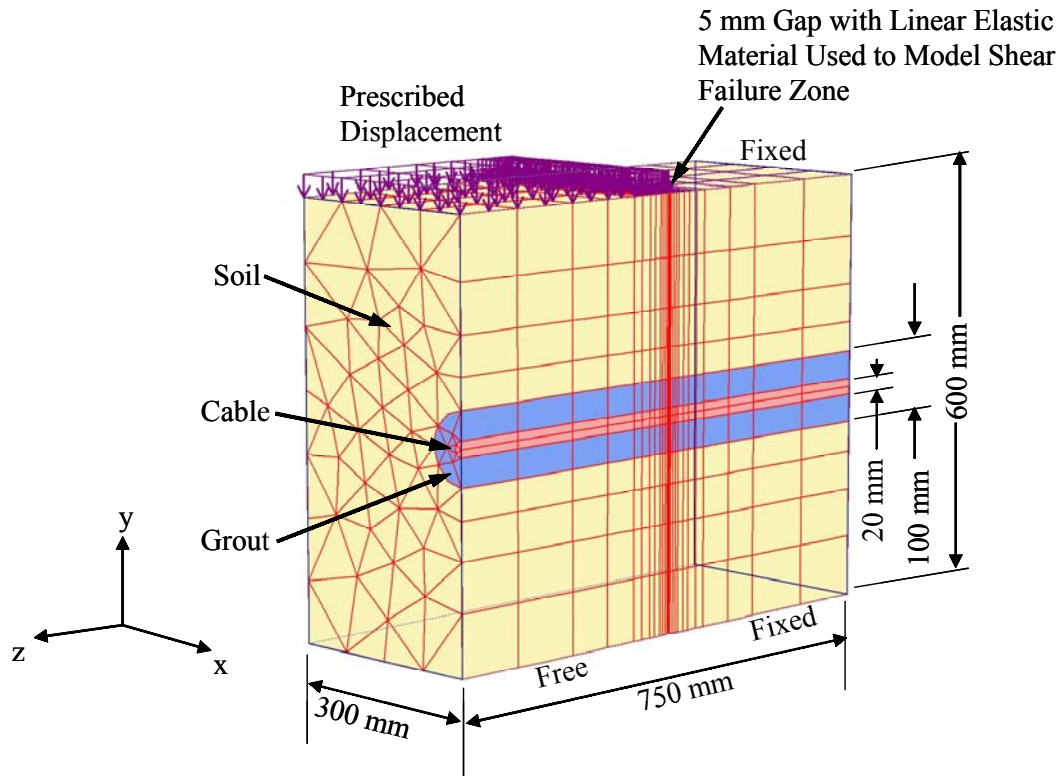
**Figure 4-2.  Three-Dimensional Model Geometry.**

To simulate the shearing soil mass a prescribed displacement is applied to the top of the slices for the left half of the model in Figure 4-2, with the bottom of these slices left free.  The top of the left soil mass was displaced downward fifteen millimeters, equal to three quarters of the cable diameter. The right half of the model is fixed at both the top and bottom of the slices.  As shown in Figure 4-2 and Figure 4-3, the halves are separated by a shear zone of 5 mm, which is modeled with a linear elastic material that is several orders of magnitude softer than the surrounding soil. For example, the Modulus of Elasticity assigned to the elastic material for all models was 100 kPa, whereas the Modulus of Elasticity for the softest soil modeled was 12,500 kPa.  Additional properties of the linear elastic material will be described in a later section.

A 100 millimeter diameter borehole was employed to define the cable-grout composite, with a cable diameter of 20 millimeters. Both of these geometrical parameters were held constant throughout the analysis. This geometry is that of composites and cables that are typically in employed in the field. The cable diameter is that of the most popular, commercially available cable and similar to that employed in laboratory testing. The soil mass is 300 millimeters wide, 600 millimeters high, and 750 millimeters long. Because of axial symmetry only an axial half of the cable-grout-soil composite need be modeled.
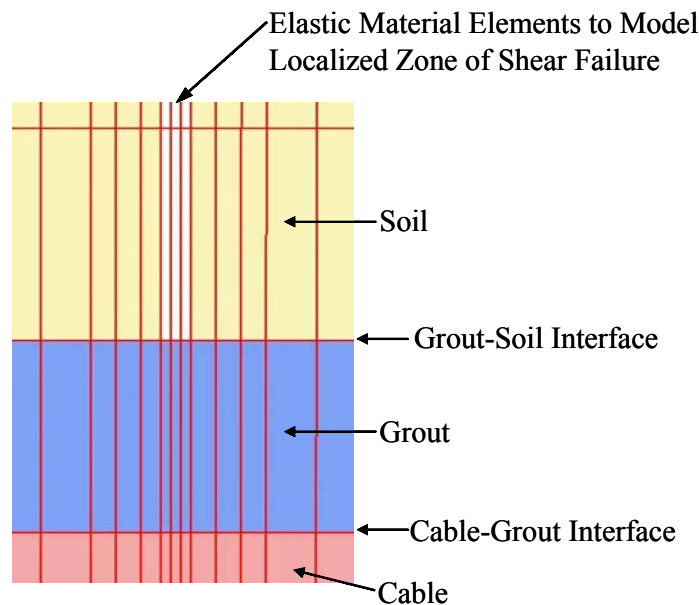


**Figure 4-3. Enlarged View of Soil Shear Zone, showing the use of linear elastic material to model the zone of shear failure in the soil.**

## Material Parameters

Many of the material parameters used in the finite element model, shown in Figure 4-2 and Figure 4-3, were backcalculated from the parametric study of laboratory results that were discussed in the previous chapter. Responses of two cable types (stiff and compliant) were studied with the finite element analysis: (1) a stiff, solid aluminum

outer conductor coaxial cable and (2) a compliant, tin/copper braided outer conductor coaxial cable. Constitutive properties (strength and stiffness) of these real cables were obtained by matching measured laboratory with finite element calculated responses. Likewise grout strengths were also obtained by matching computed and measured results, which also matched unconfined compression results. Cable and grout parameters so obtained are reported in Table 4-1. Material elements were modeled with the linear elastic-perfectly plastic, Mohr-Coulomb model, which allows for plastic deformation after meeting the failure criteria (strength).

Properties are needed for two interfaces: cable-grout interface and grout-soil interface. Interface parameters describing the strength and stiffness of the interface between the coaxial cable and grout were obtained by matching laboratory data, as discussed in Chapter 3, and are listed in Table 4-1. The interface strength and stiffness for the interface between the grout cylinder and surrounding soils are input as a fraction of the grout strength. For example, the cohesion of the interface elements between the grout and soil is one half the cohesion of the grout. Similarly, the shear moduli of the interface elements are input as one quarter of the shear modulus of the grout. Further finite element analysis shows that the resulting shear stress in the cable is insignificantly affected by varying the interface strength and stiffness between the grout and the soil from these values. Appendix A contains further discussion regarding the sensitivity of the finite element model to grout-soil interface parameters.

The shear band produced by localized shear displacement of a failing soil mass is modeled by substituting an exceedingly compliant linear elastic material for the Mohr-Coulomb soil material. As shown in Figure 4-2 and Figure 4-3 this 5 mm thick plane is

perpendicular to the axial direction of the cable. The constitutive properties of the linear

elastic material are as follows: Poisson's Ratio, $\nu=0.2$; and modulus of elasticity, E=100

kPa. The low Modulus of Elasticity, relative to the soil materials, allows for large shear

displacements in the shear zone, without exceeding any failure conditions. The friction

angle ($\phi$) and Poisson's Ratio ($\nu$) were held constant, as they were for the soil, grout, and

cable material elements. Additional parametric analysis of these parameters for the

elastic shear zone is included in Appendix A.

| Model Calibration Results - Physical Parameters | | | | | |
|---|---|---|---|---|---|
| | | Symbol | Solid Aluminum Outer Conductor | Braided Outer Conductor | |
| Cable Shearing Results | Cable Strength [1] [kPa] | $c_{cable}$ | 4,700 kPa | 1,400 kPa | |
| | Cable Modulus of Elasticity [1] [kPa] | $E_{cable}$ | 300,000 kPa | 75,000 kPa | |
| Grout and Interface Parameters | Grout Strength [1] [kPa] | $c_{grout}$ | 350 kPa | 225 kPa | |
| | Grout Modulus of Elasticity [1] [kPa] | $E_{grout}$ | 75,000 kPa | 75,000 kPa | |
| | Interface Strength [1] [kPa] | $c_{interface}$ | 90 kPa | 28 kPa | |
| | Interface Shear Modulus [1] [kPa] | $G_{interface}$ | 50 kPa | 13 kPa | |
| Critical Cable Response | Critical Cable Shear Stress [kPa] | $\sigma_{yz}$ [2] | 2000 kPa | 350 kPa | |
| | Critical Cable Slope | $\gamma_{yz}$ [2] | 0.13 | 0.065 | |
| [1] $c = (1/2){*}q_u$, $\nu=0.2$, $\phi=0°$ | | | | | |
| [2] Using Axes shown in Figure 3-1, and standard mechanics notation. | | | | | |

**Table 4-1. Material Parameters Obtained in Chapter 3.**

Optimum grout strengths for solid and braided outer conductor cables were

determined for soft to medium, medium to stiff and stiff clays. For a given soil strength

and modulus of elasticity, incremental values of grout strength were varied from 25 kPa

to 400 kPa in the TDR composite model. The soil strengths represented: (1) a soft to

medium clay [c=25 kPa], (2) a medium to stiff clay [c=50 kPa], and (3) stiff clay [c=100

kPa].   The following section describes the analysis and results from multiple

perturbations of this finite element model.



## *Finite Element Analysis and Results*

### Cable Shear Stress and Cable Slope Criteria

The deformed three-dimensional mesh after 15 mm displacement is shown in

Figure 4-4 with colorized transverse shear stresses ($\sigma_{yz}$) in the cable.  These shear stresses

in the cable are compared to the critical shear stress level criteria calculated in Chapter 3.

The greatest shear stresses in the cable occur in the region of the shear zone.

The shear stress level in the cable depends on the relative values of the strength

and stiffness of the cable, grout, and soil, as well as the magnitude of relative

displacement.   If the grout is sufficiently weaker (softer) than the cable the grout will

shear around, rather than through, the cable and not develop a large enough shear stress

level in the cable.  If the grout is too strong (stiffer) the soil adjacent to the shear band

will shear around the cable-grout composite.  Where the soil adjacent to the shear band

fails it will not deform the cable-grout composite locally enough to cause sufficient shear

stress in the cable.

A minimum shear stress or radius of curvature is required in the cable to cause

sufficient deformation to produce a TDR voltage reflection as discussed in Chapter 3.

Because the deformed zone is equal for all tests, the radius of curvature and slope of the

cable are equal.  Also, because the shear stress in the cable and the slope in the cable are

directly correlated, the cable stress rather than the slope, is reported throughout this chapter.  Results of the analysis will be discussed in the next section.
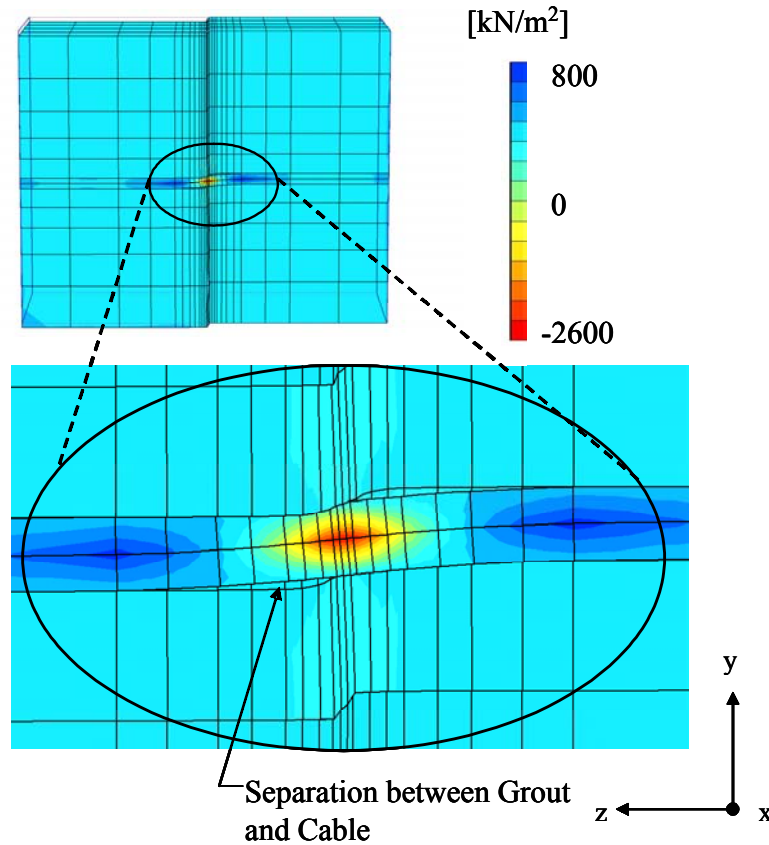


**Figure 4-4.  Example of Shear Stress ($\sigma_{yz}$) Concentration in Cable.**

**Soil and Grout Behavior**

Optimum grout strength for the two cables in a medium-stiff soil can be found from the comparison of calculated maximum shear stress in the cable as a function of the grout strength in Figure 4-5a. The optimal grout strength for a specific soil strength corresponds to region 2.   Shear stress levels in the cable that are 'less-than-optimal' correspond to regions 1 and 3.  Suboptimallity occurs for one of two reasons: (1) the grout is too compliant to shear the cable (region 1 on Figure 4-5a) or (2) the cable-grout

composite is too strong, causing the soil adjacent to the shear band to fail around the composite (region 3 on Figure 4-5a).  Critical shear stress levels to produce a minimum TDR voltage response, calculated in Chapter 3 are shown as the dashed lines in Figure 4-5a.

Consider the shear failure of the soil around the cable-grout composite, shown in region 3 of Figure 4-5a.   The extent of failure of soil around the stiff composite can be quantified by analyzing the shear strain perpendicular to the axial direction ($\gamma_{xy}$), as shown in  Figure 4-6.   A value of two percent shear strain is used as a criterion to quantify soil shear strain around the cable-grout composite.  The cable-grout composite design can be evaluated by tracking the width (in the axial direction) of the zone of two percent shear strain around the composite.  A wider zone of 2% shear strain means that more transverse, 2D 'slices' have at least  2% shear strain ($\gamma_{xy}$) in the soil mass adjacent to the grout.

Figure 4-5b compares the growth in width (in the axial direction) of the failed soil around the composite as the grout strength increases.  It grows from 5 mm at the optimum (100 kPa grout) to 200 mm for 350 kPa.  Figure 4-7 shows the progression of failed regions axially outward from the transverse shear band in the soil as model displacement increases from 0 to 15 mm, for a solid cable in stiff grout.  Shear stress levels are defined by color on the side bar and correspond to the amount of shear stress in the material, normalized to the shear strength of the material.  Red zones have reached failure stress and are shown to grow in both volume and extension outward from the transverse shear band.  Next consider the shear failure of the grout around the cable, shown in region 1 in Figure 4-5.  The grout is too weak to sufficiently deform the coaxial

cable to produce a TDR reflection signal.  Progression of shear stress failure in a weak

grout with increasing deformation is shown in Figure 4-8 to advance along the cable.

The contrast between the shear stress failure locations (red areas) in Figure 4-7

and Figure 4-8 exhibits the different causes for 'less-than-optimal' shear stress levels in

the cable.  Failure (red zones) for weak grout (region 1, Figure 4-5) in Figure 4-8 is

located predominantly in the grout.  In contrast, failure for the strong grout (region 3,

Figure 4-5) occurs in the soil.

# Medium to Stiff Soil
## $E_{soil}$=25,000 kPa, $c_{soil}$=50 kPa
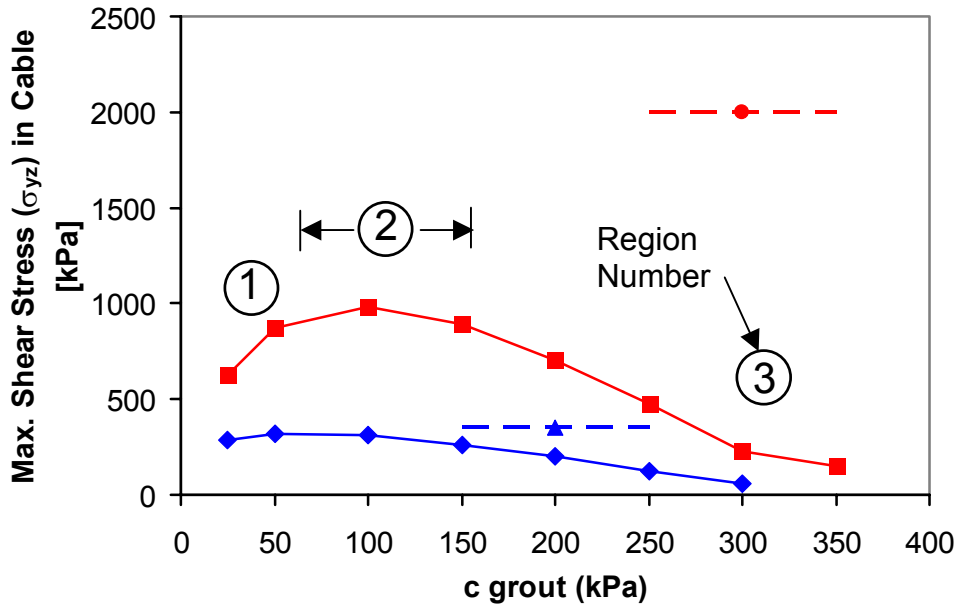


**a) Cable Shear Stress versus Grout Strength.**
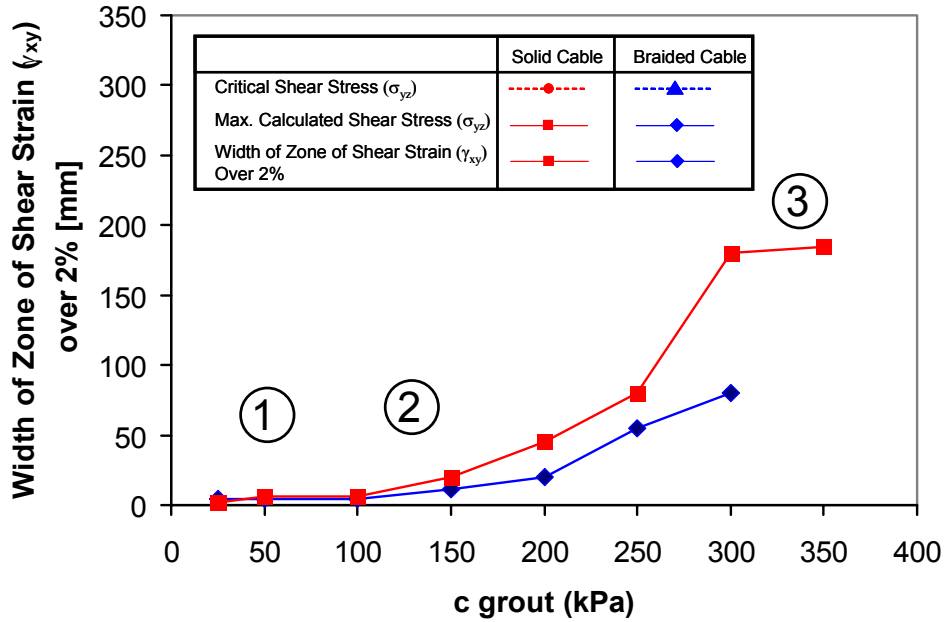


**b) Soil Shear Strain versus Grout Strength.**

**Figure 4-5. Plots of Cable Shear Stress and Width of Zone of Shear Strain over 2% Versus Grout Strength, for both Cable Types.**
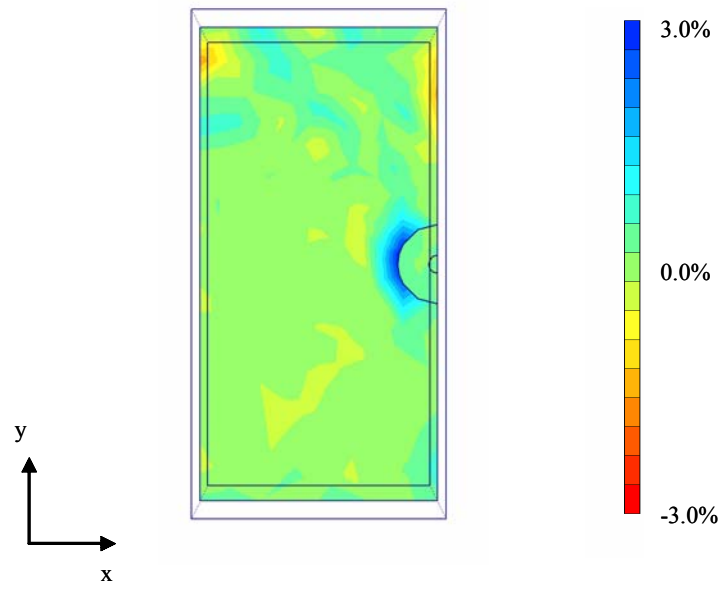
**Figure 4-6. 2-D Slice Showing Soil Shear Strain ($\gamma_{xy}$) of Soil Around Grout**
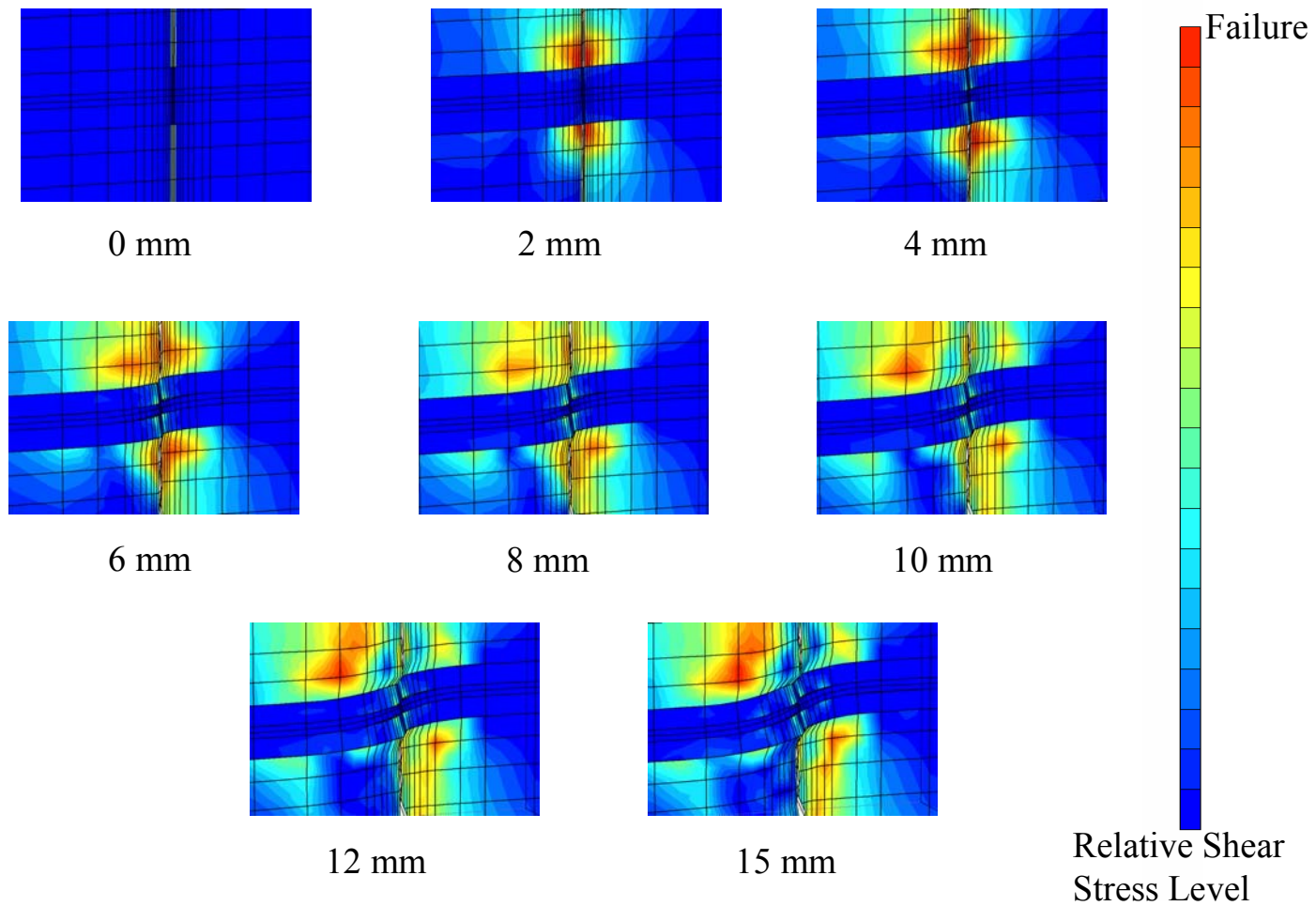
**Figure 4-7.  Progression of Shear Stress During Prescribed Displacement, for Strong Grout.**

0 mm     2 mm     4 mm

6 mm     8 mm     10 mm

12 mm     15 mm

Failure

Relative Shear
Stress Level
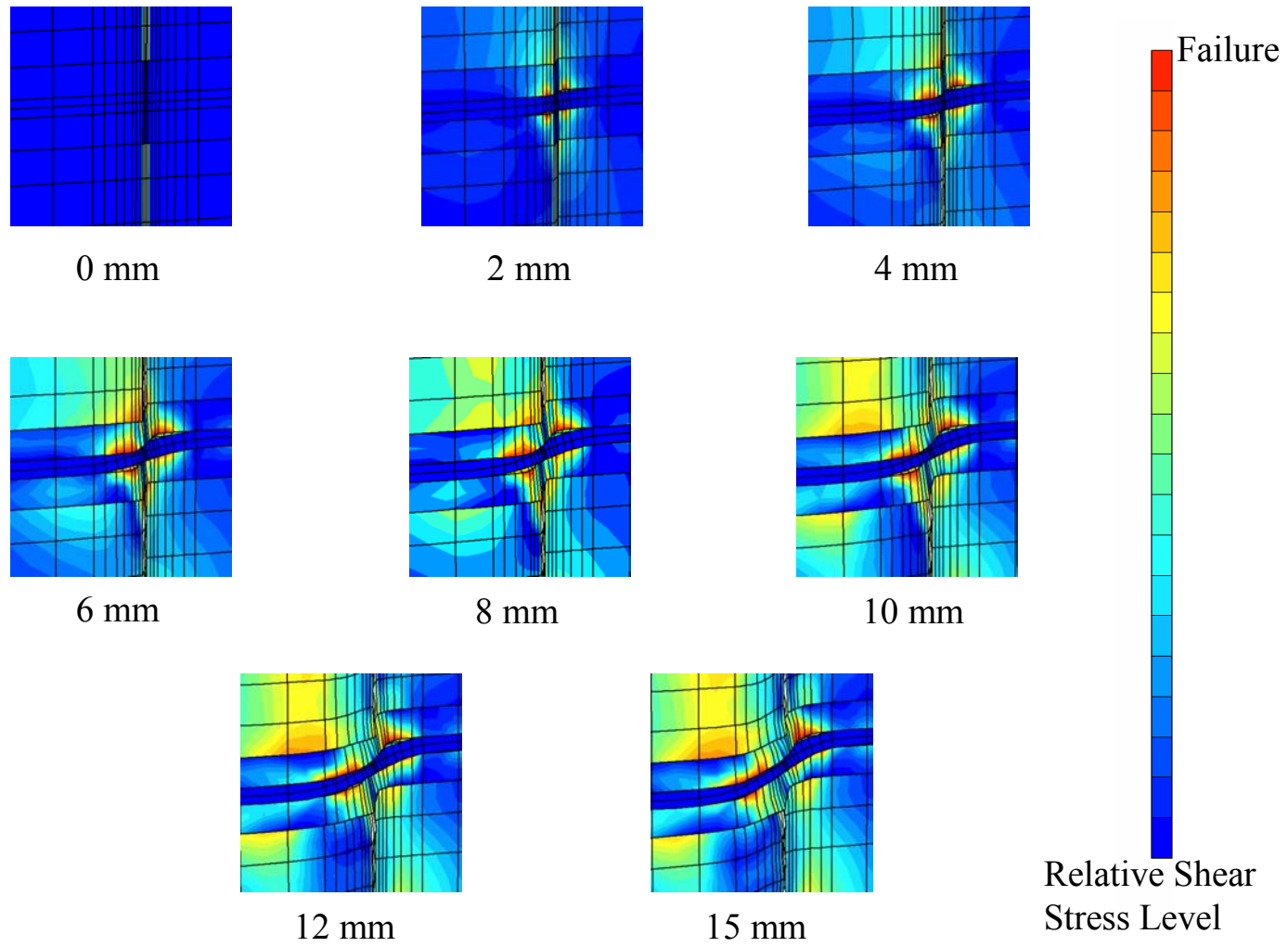
**Figure 4-8.  Progression of Shear Stress during Prescribed Displacement, for Weaker Grout.**
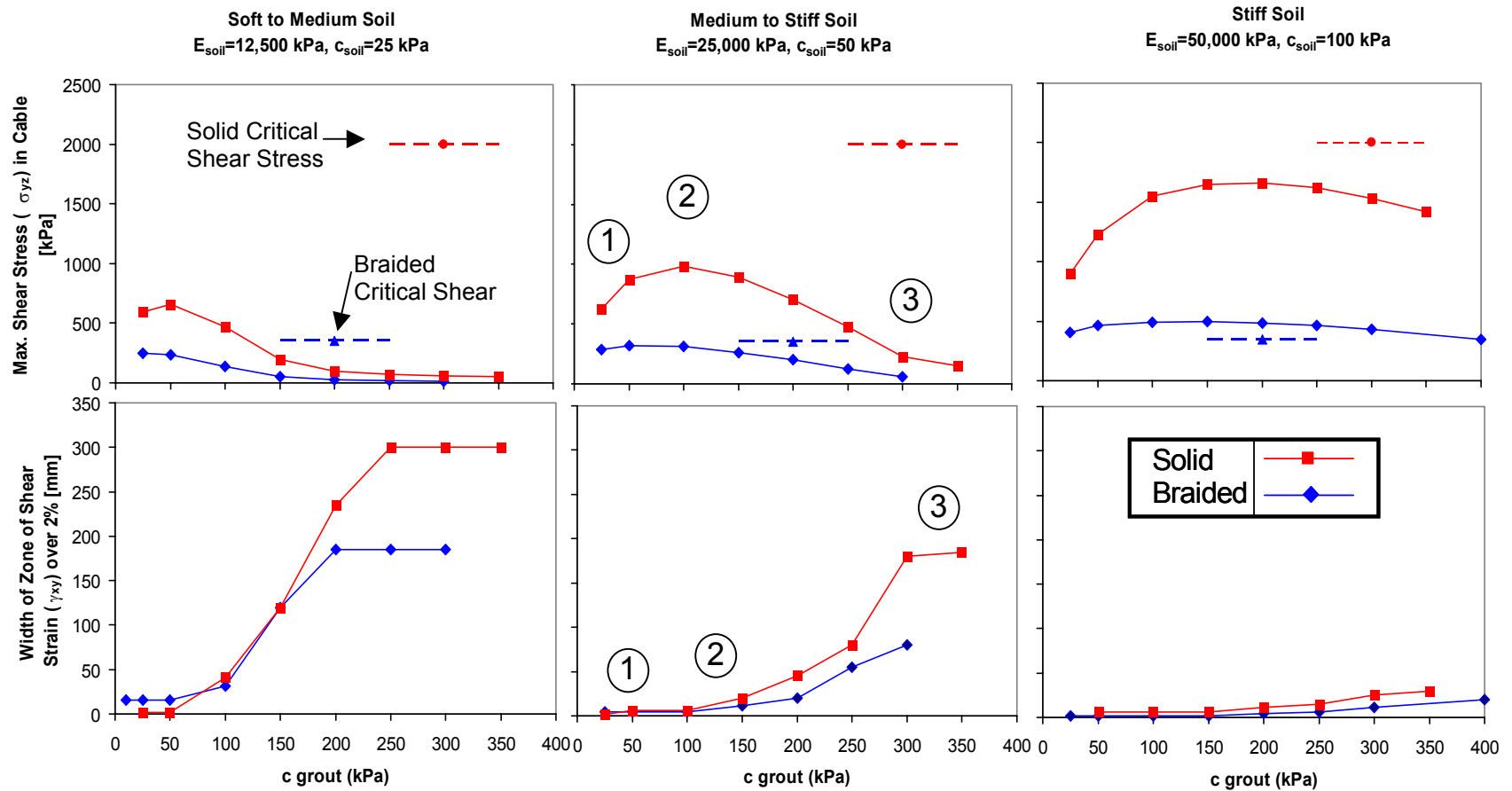
**Figure 4-9. Cable Shear Stress ($\sigma_{yz}$) and Zone of Shear Strain ($\gamma_{xy}$) over 2% versus Grout Strength, for Soft, Medium to Stiff, and Stiff Soil Strengths.**

## Cable and Grout Design

Calculated shear stress levels in the coaxial cable for both cable types (Solid and Braided) are compared in Figure 4-9 for the three soil strengths. The medium stiff soil (middle) comparison was introduced as Figure 4-5. Also shown in Figure 4-9 is the critical shear stress for each cable type, which corresponds to the shear stress necessary to generate a TDR response (see Chapter 3).

Two conclusions regarding cable and grout design for TDR applications in soils can be drawn from Figure 4-9. First, with an optimal cable-grout composite, the braided cable requires less relative displacement of the shear band to reach the critical shear stress required for TDR response. This conclusion can be drawn because additional shear displacement causes additional shear stress in both cables; the braided cable reaches critical shear stress after 15 millimeters of displacement, whereas the solid cable will require more displacement. Secondly, there is an optimal grout to soil strength (stiffness) relationship for generating shear stress in the cables. The relative displacement across the shear band was fifteen millimeters for the calculated results shown in Figure 4-9, which is important in the evaluation of cable performance. The more flexible, braided cable exceeds the critical shear stress level in the medium and stiff soil types, whereas the solid aluminum cable does not. Therefore, the braided cable appears to be more efficient for use in TDR detection of shearing in soft soils. Additional soil shear displacement will cause the shear stress levels to increase in both cables. Sensitivity of the shear stress levels to soil displacement is discussed in detail in Appendix A.

As shown in Figure 4-9, the shear stress level in the cables maximizes at optimum grout strength for each soil type.  While the data in Figure 4-9 is reported as a function of grout strength, they could also be plotted as a function of the ratio between soil and grout strength, as shown in Figure 4-10.  The optimum grout strength is 1 to 5 times the soil strength.  Realities of producing grouts in the field restrict this design suggestion to grouts with shear strengths above 250 kPa (unconfined compression strength, $q_u$ = 500 kPa), which is the weakest grout used in the field, as discussed in Chapter 3.  It is beneficial to design the grout strength as close to this relationship as possible.
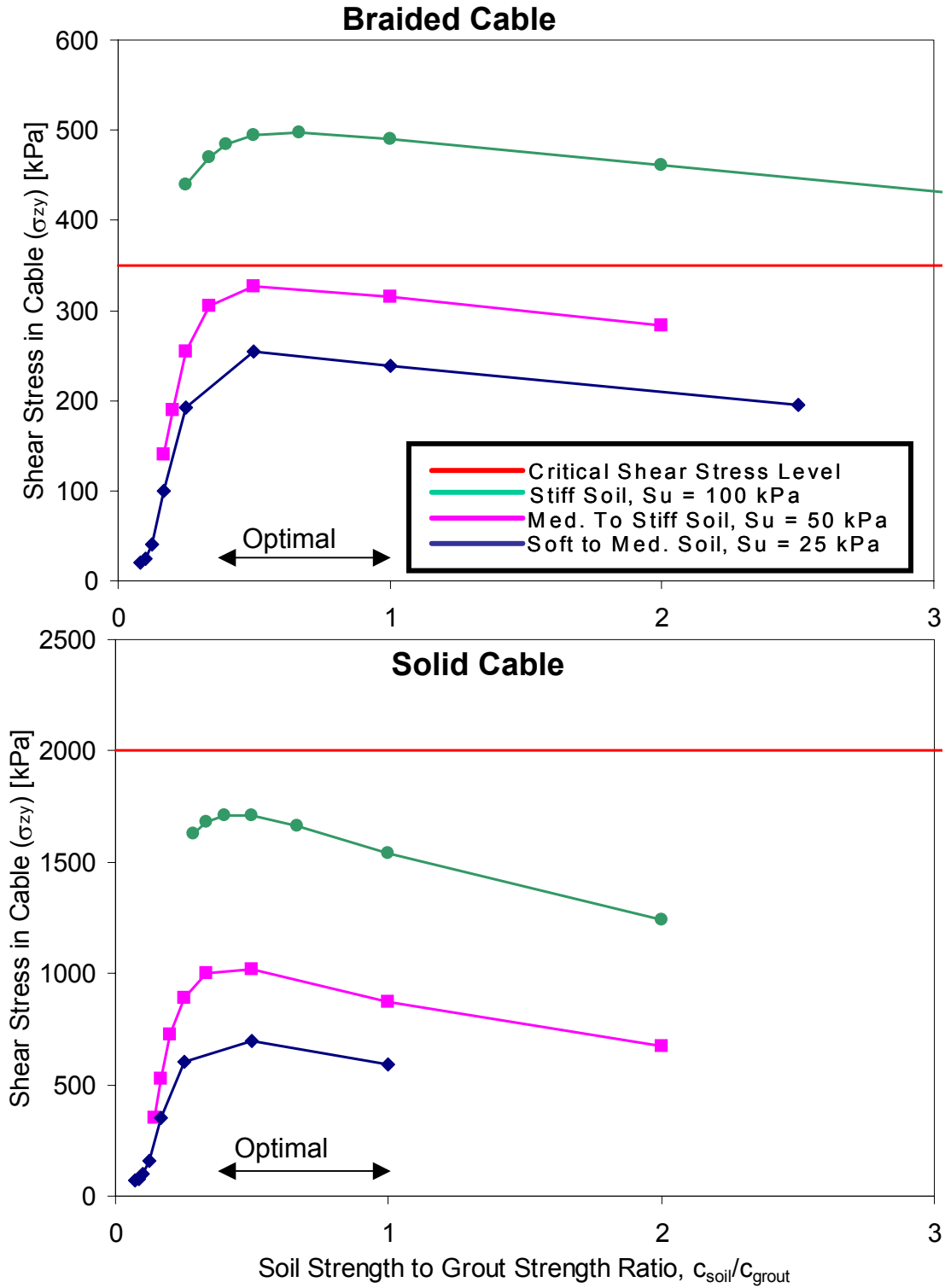
**Figure 4-10. Plots of Cable Shear Stress versus Soil Strength to Grout Strength Ratio, for both cable types.**

### *Summary*

Three dimensional finite element analysis of the elastic-plastic interaction between the soil, grout, and a Time Domain Reflectometry cable intersecting a deforming slip surface has provided insight into the behavior of each component. The analysis employed cable, grout, and cable-grout interface properties measured in the laboratory to model anticipated field conditions. The complex, three dimensional model involved three different material types (cable, grout, and soil), and two interfaces (cable-grout and grout-soil). Two realistic cables (braided and solid aluminum outer conductors), one hole size (similar in diameter for a slope inclinometer), and three soil types were investigated. The model was deformed by a prescribed displacement on one side of the slip surface or shear band. Grout strengths were varied in order to find that which sufficiently deformed the cable to produce a critical shear stress (calculated to coincide with the onset of TDR reflection). This process and the associated sensitivity studies required some 100 finite element model runs of the cable-grout composite-soil interaction.

This extended analysis showed that there is an optimum grout strength to maximize the shear stress in a given cable for a given soil strength. More specifically, the analysis has shown that more compliant, braided cables will generate a TDR response in softer soils with less displacement than the more rigid, solid aluminum cable (undergoing equal soil shear displacement). 'Less-than-optimal' conditions for TDR response occur as a result of two material conditions: (1) the grout is sufficiently stronger (stiffer) than the surrounding soil, which causes the soil to shear around, rather than through, the cable-grout composite, or (2) weak (compliant) grout lacks the strength and stiffness to cause adequate deformation of the cable for TDR response. A ratio of

grout strength to soil strength of five or less will provide optimal conditions for shearing

both cables and avoid shear displacement of soft to medium soils around the composite.

# Chapter 5.  <u>**Conclusion and Recommendations**</u>

Three-dimensional finite element analysis of laboratory shearing of: 1) TDR cable and 2) TDR cable-grout composites has resulted in parameter calibration for a range of coaxial cables and grout types.  Back-calculated grout parameters independently support the results of the finite element model of the composite, by showing the similarity between the grout strengths as back-calculated with the model and those measured in unconfined compression.  Calculated critical cable shear stress and deformation (slope) at 15 mm relative displacement are used in soil mass-composite models to provide numerical criteria necessary to interpret model results, for which there are no laboratory measurements for calibration.

Three dimensional finite element analysis of the elastic-plastic interaction between the soil-mass, grout, and a Time Domain Reflectometry cable intersecting a deforming slip surface has provided insight into the behavior of each component.  The analysis employed cable, grout, and cable-grout interface properties measured and determined in the laboratory to model anticipated field conditions.  The complex, three dimensional model involved three different material types (cable, grout, and soil), and two interfaces (cable-grout and grout-soil).  Two realistic cables (braided and solid aluminum outer conductors), one hole size (similar in diameter for a slope inclinometer), and three soil types were investigated.  The model was deformed by a prescribed displacement across the slip surface or shear band.  Grout strengths were varied in order to find that which sufficiently deformed the cable to produce a critical shear stress (calculated to coincide with the onset of TDR reflection).  This process and the associated

sensitivity studies required some 100 finite element model runs of the cable-grout composite-soil interaction.

This extended analysis showed that there is an optimum grout strength to maximize the shear stress in a given cable for a given soil strength. More specifically, the analysis has shown that with optimal grouts more compliant, braided cables will generate a TDR response in softer soils with less displacement than the more rigid, solid aluminum cable (undergoing equal soil shear displacement). 'Less-than-optimal' conditions for TDR response occur as a result of two material conditions: (1) the grout is sufficiently stronger (stiffer) than the surrounding soil, which causes the soil to shear around, rather than through, the cable-grout composite, or (2) weak (compliant) grout lacks the strength and stiffness to cause adequate deformation of the cable for TDR response. A ratio of grout strength to soil strength of five or less will provide optimal conditions for shearing both cables and avoid smearing the slip surface in soft to medium soils.

The three-dimensional finite element analysis of TDR cable-grout-soil interaction can be extended to other rigid, cylindrical inclusions in soft soils, such as soil nails and ground anchors. Additional software packages can be employed for future analysis of cable-grout-soil interaction during deformation to validate the conclusions drawn in this thesis.

## References

Cole, R.G. (1999)  Compliant TDR Cable/Grout Composites to Measure Localized Soil
Deformation, M.S. Thesis, *Department of Civil Engineering, Northwestern
University, Evanston, IL, USA*.

Brinkgreve, R.B.J. and Vermeer, P.A. (2001) Plaxis 3D Tunnel Version 1 Manual, A.A.
*Balkema Publishers, Lisse, Netherlands*.

Bilane, C. (1994)  Effects of Multiple Crimps and Cable Length on Reflection Signatures
from Long Cables, M.S. Thesis, *Department of Civil Engineering, Northwestern
University, Evanston, IL, USA.*

CommScope Inc (1998), "Cable Products Catalog," *North Carolina*

Dowding, C.H. and Huang, F.C. (1994), "Early Detection of Rock Movement with Time
Domain Reflectometry", *Journal of Geotechnical Engineering*, ASCE, August.

Dowding, C.H., Cole, R.G., Pierce, C.E. (2001) "Detection of Shearing in Soft Soils with
Compliantly Grouted TDR Cables",  Proceedings TDR 2001, C.H. Dowding Ed.,
*Infrastructure Technology Institute, Northwestern University, Evanston, IL USA,
ISBN 0-9712631-0-8.*

Dowding, C.H. (1994) Time Domain Reflectometry for Landslide Surveillance,
Proceedings, Landslides: Causes, Impacts, and Countermeasures, H.H. Einstein
et.al. Eds., *United Engineering Foundation, New York, NY, USA.*

GAI Consultants, 570 Beatty Rd., Monroeville, PA 15146; Field Data, *Personal
Communication.*

O'Connor, K.M. and Dowding, C.H. (1999), Geomeasurements by Pulsing TDR Cables and Probes, *CRC Press, New York, NY, USA.*

O'Connor, K.M. (1998), "Installation of TDR Monitoring Cables, Clark Landfill, Indiana," *GeoTDR, Inc. Report.*

## Appendix A.    <u>Parameter Sensitivity Analysis</u>

The sensitivity of calculated cable and cable-grout response to changes in composite material constitutive properties, model geometry, and prescribed displacement in the finite element modeling process is discussed in this section.  Parametric sensitivity studies of the finite element models in this appendix include those of: 1) laboratory cable shearing, 2) laboratory cable-grout composite shearing, and 3) cable-grout composite-soil interaction.

As discussed in Chapter 3, laboratory shear tests were conducted to determine the physical properties of cables, grout, and cable-grout interfaces commonly used in Time Domain Reflectometry (TDR) measurements.  These laboratory shear tests were modeled with finite elements and backcalculated constitutive properties were used for further finite element analysis of TDR cable-grout composite-soil interaction.  Constitutive properties that were held constant throughout the modeling  of laboratory tests are the friction angle of the cable and grout ($\phi=0°$) and the Poisson ratio of the cable and grout ($v=0.2$).  Various interface strength and stiffness parameter values were employed throughout the FEM process, which are discussed in Chapters 3 and 4.

Many constitutive properties were assigned constant values throughout the finite element analysis of the TDR cable-grout composite-soil interaction.  These parameters include:  three moduli of elasticity, E  (grout, soil, and elastic material used to model shear zone in soil), three Poisson Ratios, $v$ (soil, grout, and elastic shear zone material), friction angle of soil and grout ($\phi$), and interface strength between grout and soil. The sensitivity of the results to these parameters can be analyzed by comparing calculated

cable shear stress versus grout strength curves for variations of these parameters. Similarly, by comparing the calculated curves for larger and smaller soil masses and larger and smaller prescribed displacements the sensitivity of the cable shear stress to these factors also can be analyzed.

## *Models of Laboratory Shearing – Parametric Sensitivity Analysis*

### Cable Shear Test

The constitutive properties of cables commonly used in TDR were acquired by matching finite element calculated force-displacement curves with those measured in laboratory shearing, as discussed in Chapter 3. The modulus of elasticity and cohesion of the cable were used as variable parameters throughout the curve fitting process; however, the Poisson ratio and friction angle were held constant at 0.2 and zero degrees, respectively. Figure A-1 and Figure A-2 show the various force-displacement curves for the solid aluminum cable when only the Poisson ratio (A-1) or friction angle (A-2) is changed. As shown, changing either the Poisson ratio or friction angle has little effect on the calculated force-displacement results. Because there are no initial normal stresses or internal body stresses in the cable, it is expected that changing the friction angle would have little effect on the final results.
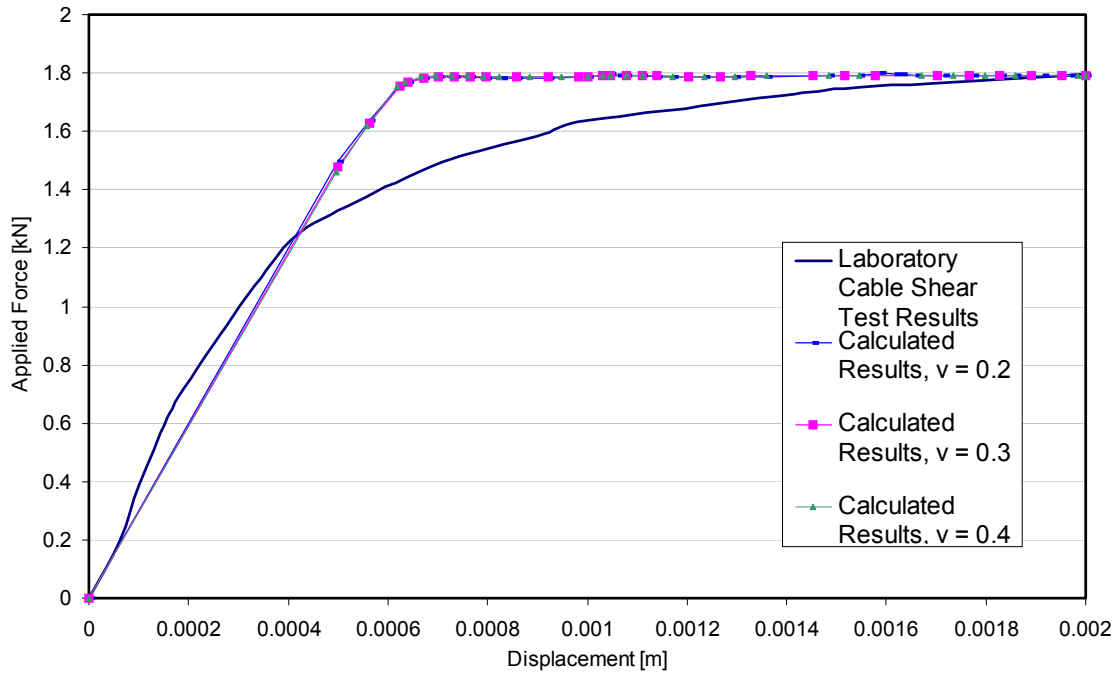
**Figure A-1. Calculated and measured force-displacement curves for cable shear test, as discussed in Chapter 3, for different cable Poisson ratios. All other parameters were held constant, including: cohesion (c=4,700 kPa), elastic modulus (E=300,000 kPa), and friction angle ($\phi$=0º).**

**Cable Shear Test Results-Solid Aluminum Cable with Different Cable Friction Angle Values:  c = 4,700 kPa, E=300,000 kPa, ν = 0.2**
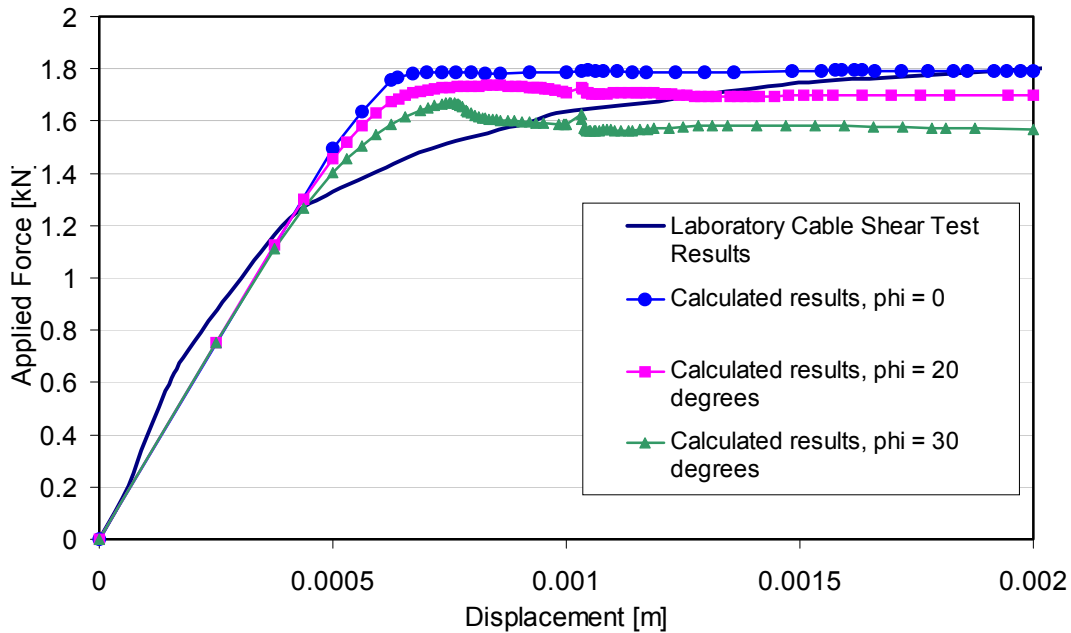


**Figure A-2. Calculated and measured force-displacement curves for cable shear test, as discussed in Chapter 3, for different cable friction angles.  All other parameters were held constant, including: cohesion (c=4,700 kPa), elastic modulus (E=300,000 kPa), and Poisson Ratio (ν=0.2).**

**Cable-Grout Composite Shear Test**

After obtaining the appropriate cable parameters, grout parameters are acquired by matching the measured force-displacement curves from the cable-grout composite shear test, as discussed in Chapter 3.  The measured force-displacement curves were matched with calculated curves by changing the elasticity modulus and cohesion parameters of the grout.  The strength and stiffness of the interface between grout and soil were also variable throughout the curve fitting procedure, as discussed in Chapter 3. Once the appropriate modulus of elasticity, cohesion, and interface properties were

acquired, the sensitivity of the results to a change in friction angle and Poisson ratio was analyzed. The calculated force-displacement curves with various friction angles and Poisson ratios are shown in Figure A-3 and Figure A-4, respectively. By increasing the grout friction angle to twenty degrees the applied force required to reach a plastic deformation increased by approximately ten percent, however the computation time increased dramatically, therefore zero degrees was used as the grout friction angle. Because there is minimal initial normal stress or body stresses in the composite, it is expected that that friction angle would have little effect on the results. As shown in Figure A-4, varying the grout Poisson ratio had little effect on the calculated force-displacement curves.
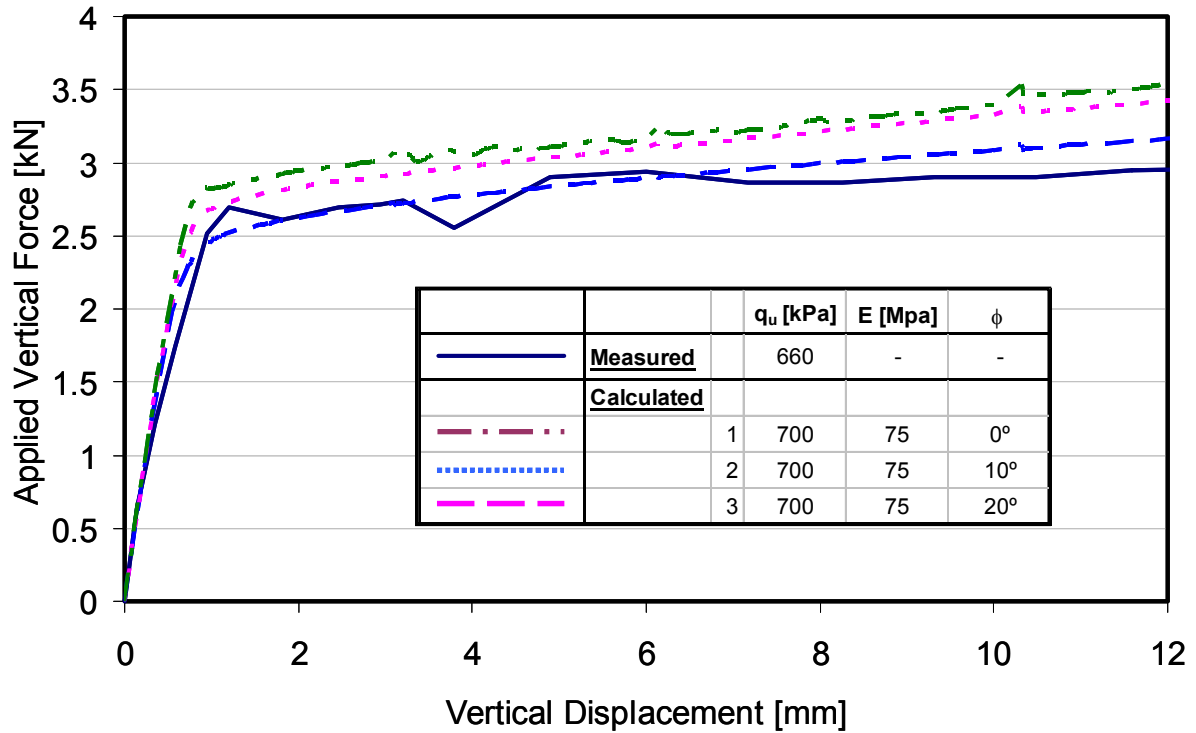
**Figure A-3. Calculated and measured force-displacement curves for composite shear test, as discussed in Chapter 3, for different grout friction angles. The grout properties (unconfined compression strength, elastic modulus, and varying friction angles) are listed in the table above. The grout Poisson ratio is constant ($\nu_{grout} = 0.2$). The cable parameters are held constant, including: cohesion ($c_{cable} = 4,700$ kPa), elastic modulus ($E_{cable} = 300,000$ kPa), Poisson ration ($\nu_{cable}=0.2$) and friction angle ($\phi_{cable}=0^o$).**

| | | | $q_u$ [kPa] | E [Mpa] | $\nu$ |
|---|---|---|---|---|---|
| ——— | **Measured** | | 660 | - | - |
| | **Calculated** | | | | |
| —·—··— | | 1 | 700 | 75 | 0.2 |
| ·············· | | 2 | 700 | 75 | 0.3 |
| — — — | | 3 | 700 | 75 | 0.4 |
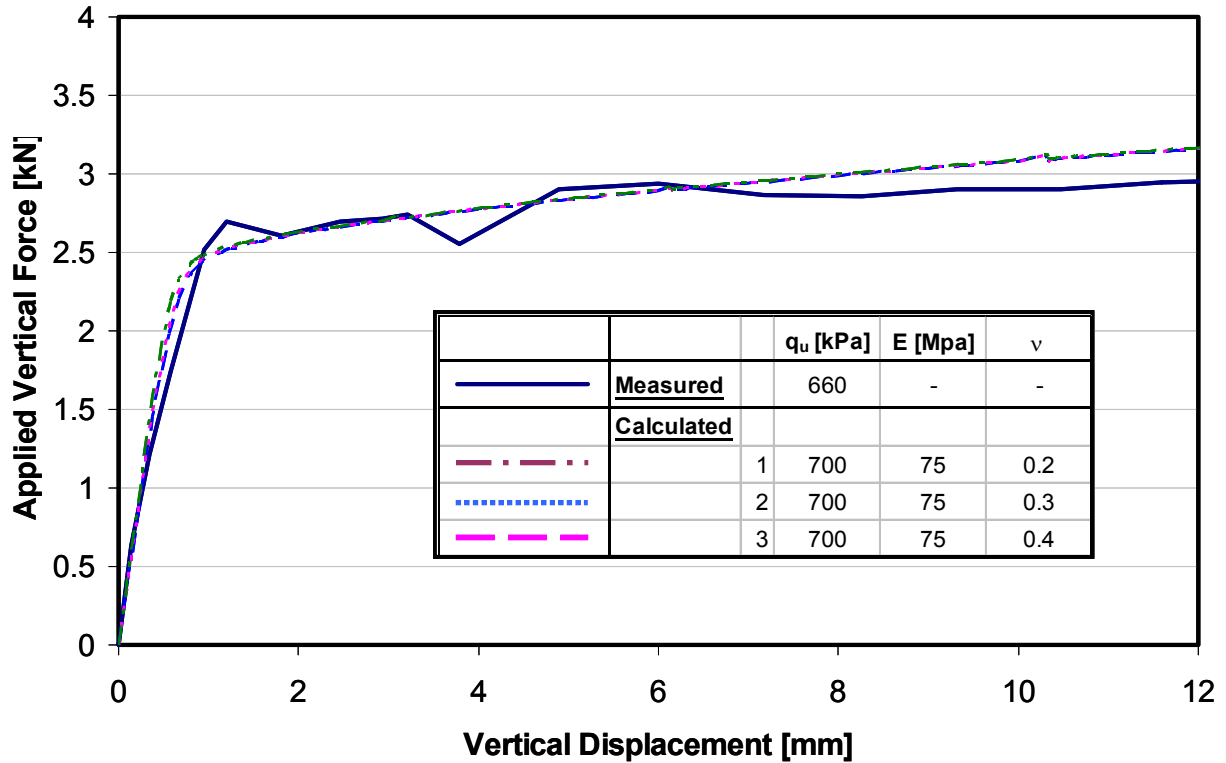
**Figure A-4. Calculated and measured force-displacement curves for composite shear test, as discussed in Chapter 3, for different grout Poisson Ratio values. The grout properties (unconfined compression strength, elastic modulus, and varying Poisson ratios) are listed in the table above.  The grout friction angle is constant ($\phi_{grout}$ = 0º).  The cable parameters are held constant, including: cohesion ($c_{cable}$ = 4,700 kPa), elastic modulus ($E_{cable}$ = 300,000 kPa), Poisson ration ($\nu_{cable}$=0.2) and friction angle ($\phi_{cable}$=0º).**

## _Cable-Grout Composite-Soil Interaction Analysis – Parametric Sensitivity Analysis_

### Shear Zone Constitutive Properties

The linearly elastic material used to model the soil shear zone during the finite element analysis was assigned the following parameters:  Poisson Ratio, $\nu$ = 0.2; modulus of elasticity, E = 100 kPa.  The modulus of elasticity was chosen to be sufficiently

compliant (softer) than that of the surrounding soil.   For example, the softest soil modeled was assigned a modulus of elasticity of 12,500 kPa, which is over an order of magnitude greater than that for the shear zone.  The Poisson ratio, $\nu$, is equal to that of the soil, grout, and cable ($\nu=0.2$).

Changing the Poisson Ratio of the shear zone material minimally affects the calculated shear stress level in the cable and does not affect the optimal grout strength. Figure A-5 shows the calculated cable shear stress ($\sigma_{yz}$) versus grout strength curves for different Poisson ratio values, with all other parameters being held constant.  As reported in Chapter 3, a value of 0.2 was used throughout the finite element analysis.   By increasing the Poisson Ratio by over one hundred percent, the maximum shear stress in the cable increases by only fifteen percent.  Although the change in elastic material Poisson ratio affects the shear stress level in the cable, the optimal grout strength, where the cable shear stress peaks, does not change.

Figure A-6 shows the calculated cable shear stress versus grout strength curves for different Modulus of Elasticity values.  By decreasing the modulus of elasticity for the shear zone by 50 percent, the maximum shear stress in the cable increases by 42 percent.  This increase in cable shear stress from decreasing shear zone stiffness is an important factor for future finite element modeling of TDR composite-soil interaction.  A decrease in elastic modulus significantly increases the maximum shear stress in the cable, increasing the likelihood of attaining the critical shear stress value necessary for TDR response.   Although calculated shear stress values are sensitive to modulus, the grout strength that produces the maximum shear stress in the cable is unchanged; therefore the optimal grout design remains unchanged.
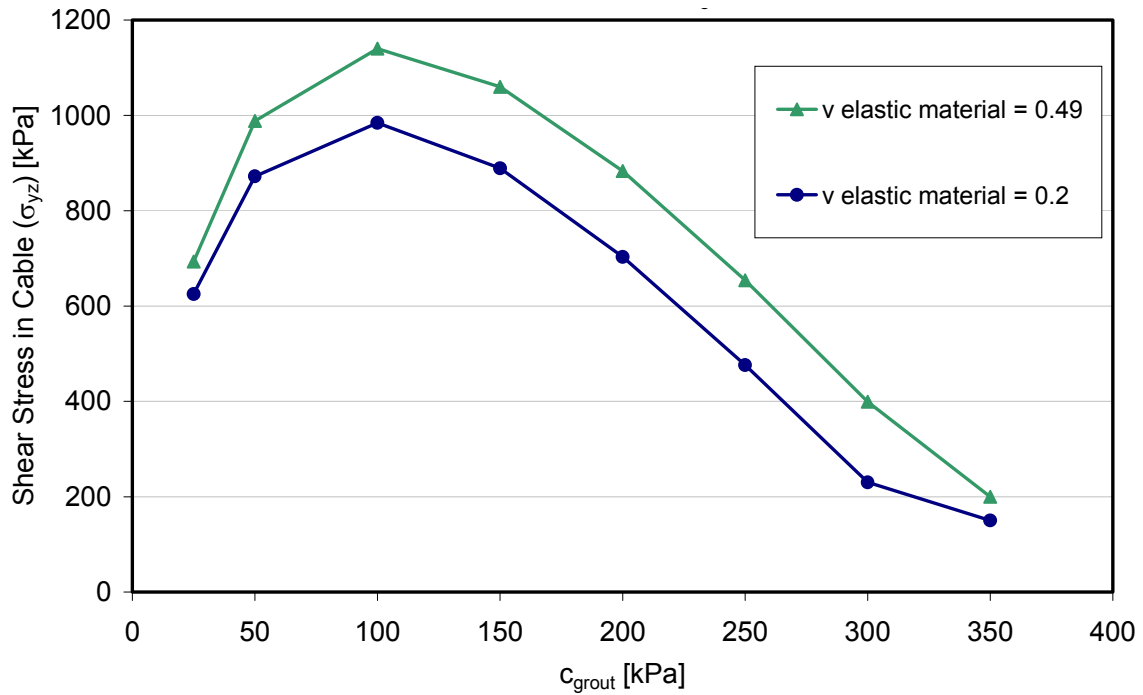
**Figure A-5. Comparison of Calculated Cable Shear Stress versus Grout Strength for Poisson Ratios of 0.2 and 0.49 in Linear Elastic Material. Parameters that are held constant include: soil strength ($c_{soil}$ = 50 kPa), soil stiffness ($E_{soil}$ = 25,000 kPa), grout stiffness ($E_{grout}$ = 75,000 kPa), soil and grout Poisson ratio ($\nu_{grout}$ = $\nu_{soil}$ = 0.2), and friction angles ($\phi_{soil}$=$\phi_{grout}$=$\phi_{cable}$=0°).**
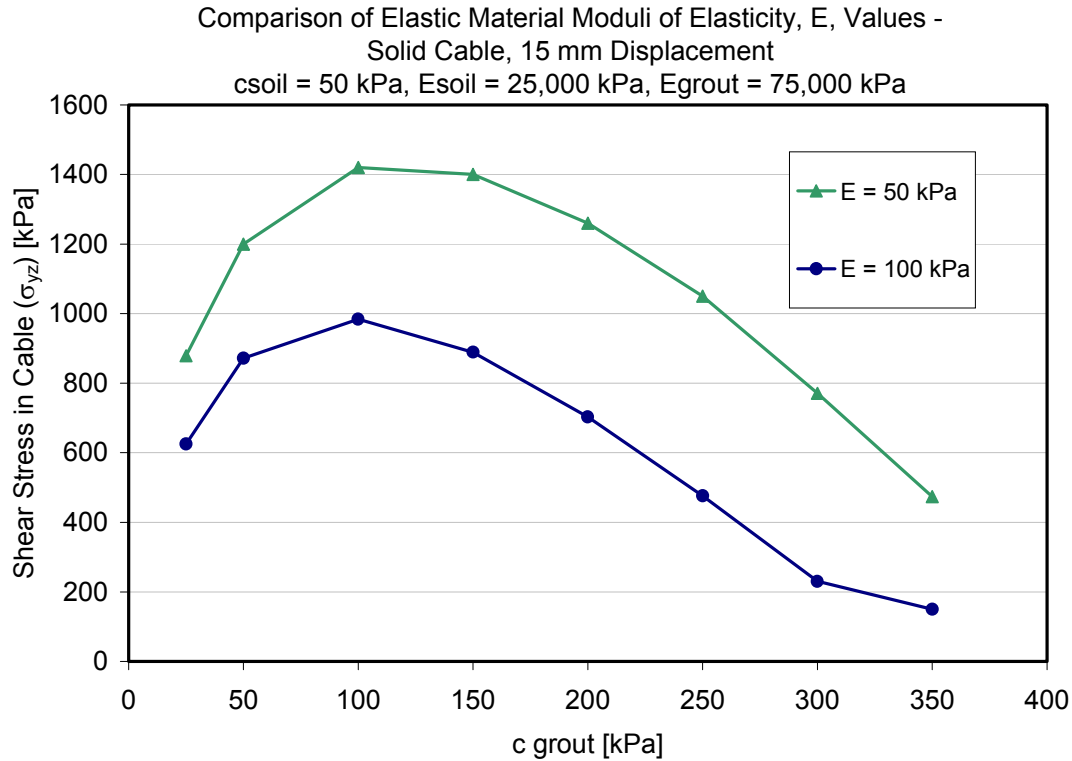
**Figure A-6. Comparison of calculated Shear Stress in Cable for Modulus of Elasticity values of 50 kPa and 100 kPa, for the linear elastic material used to model the shear band. Parameters that are held constant include: surrounding soil strength ($c_{soil}$ = 50 kPa), soil stiffness ($E_{soil}$ = 25,000 kPa), grout stiffness ($E_{grout}$ = 75,000 kPa), soil and grout Poisson ratio ($\nu_{grout}$ = $\nu_{soil}$ = 0.2), and friction angles ($\phi_{soil}$=$\phi_{grout}$=$\phi_{cable}$=0°).**

## Soil Constitutive Properties

The soil parameters that remained constant through the finite element analysis were the Poisson ratio, $\nu$=0.2, and the friction angle, $\phi$=0°. An addition to these parameters, the modulus of elasticity was given a value of 500 times the soil cohesion. For example, a modulus of elasticity of 12,500 kPa was given to the weak soil having a cohesion of 25 kPa. As shown in Figure A-7, an increase in the Poisson ratio of the soil mass does not affect the calculated shear stress in the cable. Figure A-8 shows the calculated cable shear stress curves for two values of soil modulus of elasticity, with all other parameters held constant. The soil cohesion is 50 kPa in this example, therefore the

elasticity modulus to soil cohesion ratios are 500 and 1000 for modulus values of 25,000

kPa and 50,000 kPa respectively. Increasing the modulus of elasticity by one hundred

percent causes a nine percent decrease in maximum calculated cable shear stress. The

finite element model fails due to calculation problems when a friction angle other than

zero is used. Thus a constitutive model was employed with a zero friction angle, which is

consistent with the clayey nature of typical soft soil.
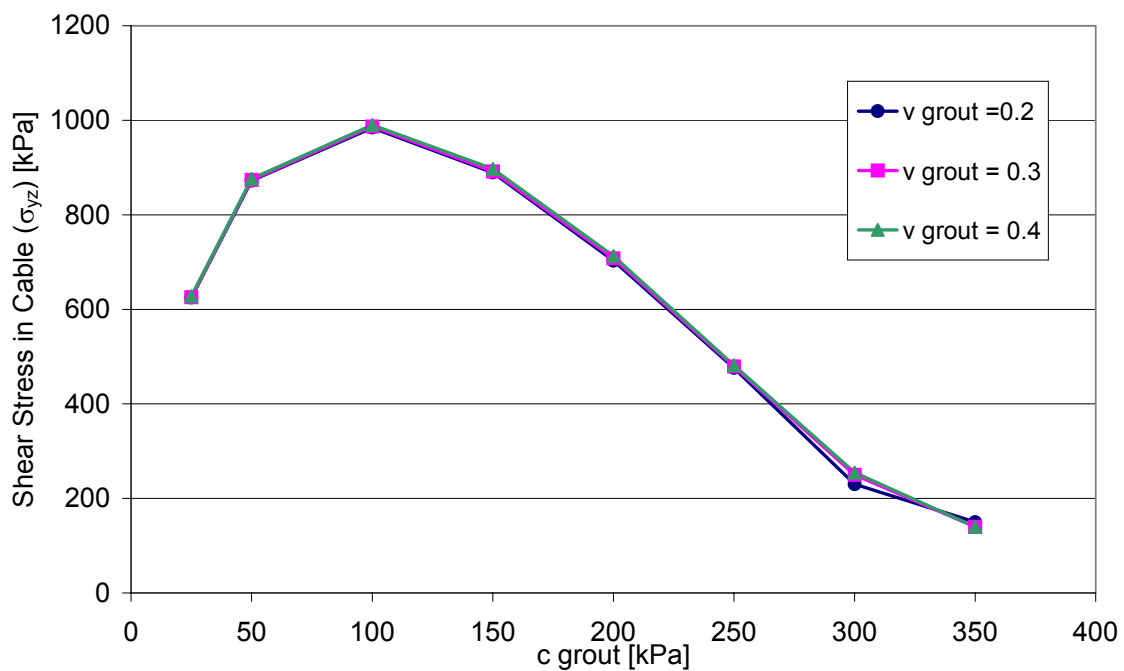


**Figure A-7. Cable shear stress versus grout strength, for different Poisson ratio values of the soil mass. Constant parameters include: all cable parameters, soil strength ($c_{soil}$ = 50 kPa), soil stiffness ($E_{soil}$ =25,000 kPa), grout stiffness ($E_{grout}$ = 75,000 kPa), grout and soil friction angle ($\phi_{grout}$=$\phi_{soil}$=0º), and grout Poisson ratio ($\nu_{grout}$=0.2).**
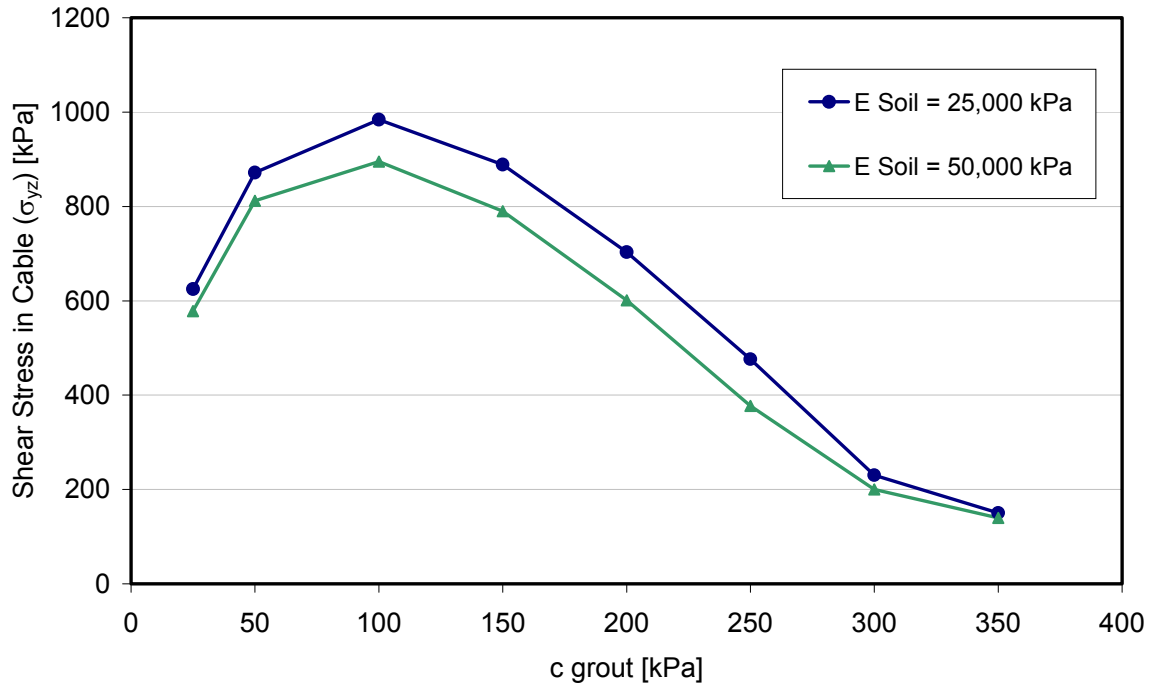
**Figure A-8. Cable Shear Stress Curves for different soil moduli of elasticity. Constant parameters include: all cable parameters, soil strength ($c_{soil}$ = 50 kPa), grout stiffness ($E_{grout}$ = 75,000 kPa), grout and soil friction angle ($\phi_{grout}=\phi_{soil}=0^o$), and grout and soil Poisson ratios ($\nu_{grout}=\nu_{soil}=0.2$).**

## Grout Constitutive Properties

Grout parameters that were held constant throughout the finite element analysis of the TDR composite-soil interaction were the friction angle, $\phi$, the Poisson ratio, $\nu$, and the modulus of elasticity, E. The friction angle was assigned a value of zero degrees, allowing for a direct relationship between the cohesion and strength of the grout. A value of 75,000 kPa was used for the modulus of elasticity and 0.2 for the Poisson ratio for the grout. Figure A-9 shows that no change occurs in the calculated cable shear stress when the Poisson ratio of the grout is changed. Similarly, changing the elastic modulus of the grout had little effect on the calculated shear stress in the cable, as shown in Figure A-10. Calculation errors occur when a friction angle other than zero degrees is used.
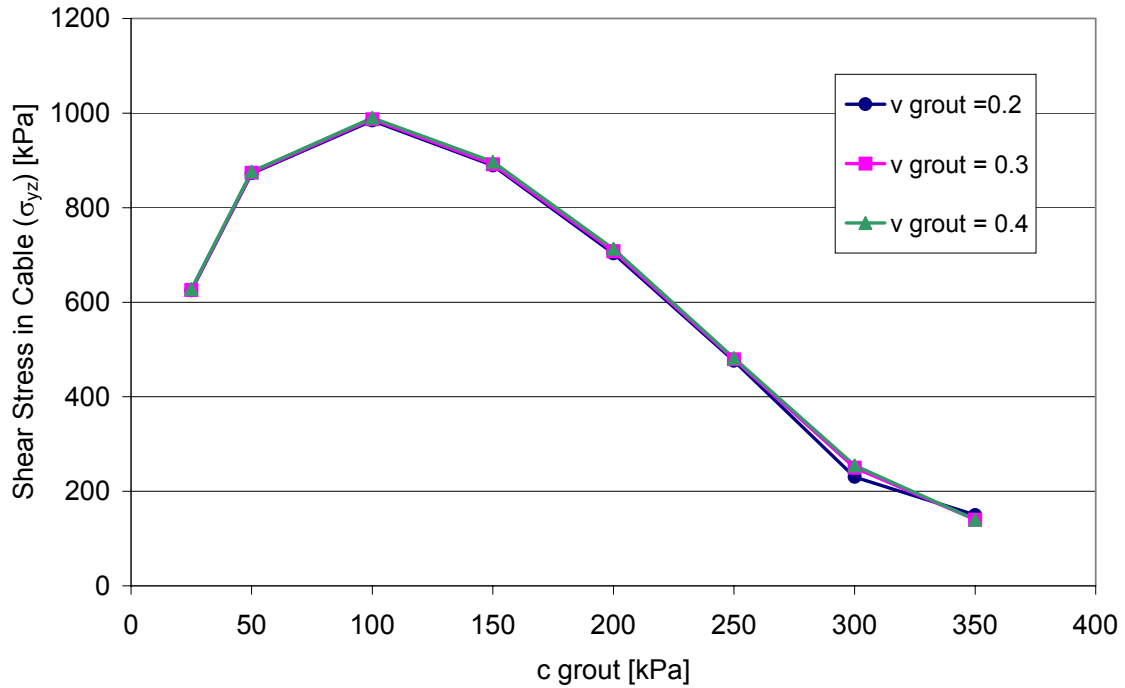
**Figure A-9. Calculated cable shear stress versus grout cohesion for different grout Poisson Ratios. Constant parameters include: all cable parameters, soil strength ($c_{soil}$ = 50 kPa), soil stiffness ($E_{soil}$ = 25,000 kPa), grout stiffness ($E_{grout}$ = 75,000 kPa), grout and soil friction angle ($\phi_{grout}=\phi_{soil}=0^o$), and soil Poisson ratios ($\nu_{soil}$=0.2).**
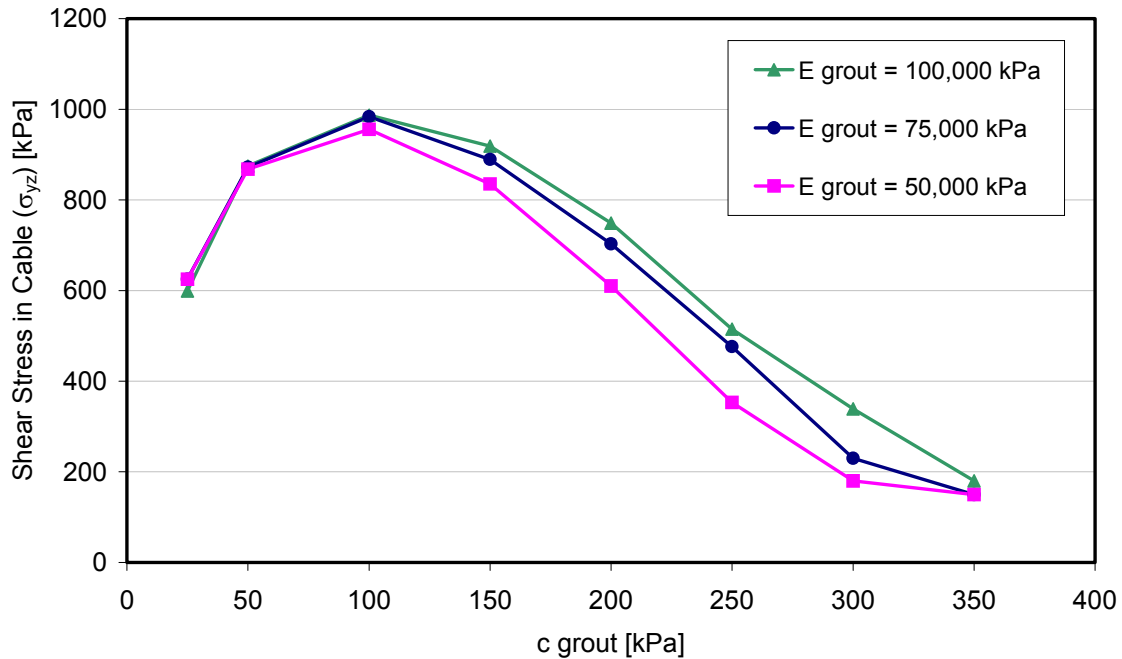
**Figure A-10. Calculated cable shear stress versus grout strength, using various grout elasticity moduli. Constant parameters include: all cable parameters, soil strength ($c_{soil}$ = 50 kPa), soil stiffness ($E_{soil}$ = 25,000 kPa), grout and soil friction angle ($\phi_{grout}$=$\phi_{soil}$=$0^o$), and grout and soil Poisson ratios ($\nu_{soil}$=$\nu_{grout}$=0.2).**

## *Summary*

The sensitivity analysis discussed above illustrates the nominal effects produced by changes in constitutive properties or material parameters. Although the calculated values of shear stress in the cable are affected by changes in material parameters, the optimal grout strength is not affected. This sensitivity analysis validates the conclusions drawn in Chapter 4, because the optimal grout strength value is not affected by parametric variation.